HYDRAULICS OF RIVER FLOW UNDER ARCH BRIDGES

REPORT NO. 3

SEPTEMBER 1960

NO. 17

Joint Highway Research Project

by

P. F. BIERY

J. W. DELLEUR

PURDUE UNIVERSITY
LAFAYETTE INDIANA

Progress Report No. 3

Hydraulics of River Flow Under Arch Bridges

TO: K. B. Woods, Director
Joint Highway Research Project

September 21, 1960

FROM: H. L. Michael, Assistant Director
Joint Highway Research Project

File: 9-6-2
Project: C-36-62H

Attached is Progress Report No. 3 "Hydraulics of River Flow Under Arch Bridges" by P. F. Biery and J. W. Delleur of our staff. This report is a summary of the findings of the research project on arch bridges which as an HPS study has been in progress since January 1, 1958.

The authors also propose to present the attached report as a technical paper at the October meeting of the American Society of Civil Engineers in Boston. The report will, after approval for such release by the Board, also be forwarded to the State Highway Department of Indiana and the Bureau of Public Roads for their review and approval for presentation at the Boston meeting.

The report is presented to the Board for information and release.

Respectfully submitted,

Harold L. Michael

Harold L. Michael, Secretary

HLM:kmc

Attachment

cc: F. L. Ashbaucher
J. R. Cooper
W. L. Dolch
W. H. Goetz
G. A. Hawkins (M. B. Scott)
F. F. Havey
G. A. Leonards
R. D. Miles
R. E. Mills
J. F. McLaughlin
C. E. Vogelgesang
J. L. Waling
J. E. Wilson
E. J. Yoder

Report No. [illegible]

Hydraulics of [illegible]

by

[illegible]
[illegible]
and
J. [illegible] DeLleur
[illegible] Prof. of Hydraulic Engineering

[illegible]
Project [illegible] 36-62
File [illegible] 9-8-2

Purdue University
Lafayette, Indiana

September, 1960

[illegible]

[illegible] system [illegible]

[illegible]

[illegible] years, [illegible]

[illegible] it is the job of the highway engineer to provide the [illegible] span [illegible] and hydraulic and economic reasons, and yet allow a [illegible] enough [illegible] information [illegible] to make an intelligent estimate of the maximum backwater [illegible] design results in making the cost of the bridge prohibitive or the [illegible] of causing flood damage excessive.

In the past, studies by the U.S. Geological Survey and the Bureau of Public Roads pertaining to backwater effects caused by constrictions have considered shapes of openings such [illegible] bridges

[illegible]

However, very little has been done in the way of making a systematic study of the hydraulics of river flow under the various shapes of arch bridges. The arch is unique in that the surface width within the barrel of the arch decreases with a corresponding increase in stage. The purpose of this research is therefore to study the hydraulics of arch bridges so as to compensate for the loss of efficiency at high flows, and to provide a method for computing the backwater upstream of the bridge. In addition, a practical method of making indirect measurements of flood flows at arch bridges is proposed.

A project was initiated in the Hydraulics Laboratory at Purdue University to study this problem. It is sponsored by the Indiana State Highway Department in cooperation with the U.S. Bureau of Public Roads.

HISTORY:

The earliest systematic laboratory investigation of flow through contractions in open channels was performed by E. W. Lane.[1*] He related the discharge and the water surface elevation through the contraction by means of empirical discharge coefficients, and indicated that there may exist some relationship between these coefficients and the ratio of the maximum backwater depth produced by the contraction to the normal depth of flow without the contraction. This ratio is referred to as the backwater ratio.

In 1955, Kindsvater and Carter[2] presented a practical solution of the discharge equation by an extensive experimental investigation. By applying correction terms for various geometric conditions to a standard discharge coefficient, the method can be applied to a wide variety of boundary conditions. A detailed description of the internal and external flow characteristics was given.

In the same year H. J. Tracy and R. W. Carter[3] presented a companion paper to the one by Kindsvater and Carter. In it they gave a method of computing the nominal backwater due to open-channel constrictions. The practical solution was based upon empirical discharge coefficients and a laboratory investigation of the influence of channel roughness, channel shape, and constriction geometry. Their study was limited to single span, deck-type constrictions and to steady, tranquil flow. C. F. Izzard,[4] in his discussion of this paper, pointed out that the backwater ratio is definitely a function of the normal depth Froude number at the constricted section. Also he questioned the use of the backwater ratio concept when the head loss between the section of maximum backwater and the vena contracta is large compared to the approach velocity head.

The combined work of Kindsvater, Carter, and Tracy was organized into a U.S. Geological Survey Circular,[5] which presented a method for determining peak discharges at abrupt contractions. The discharge estimate was to be made from a survey of high-water marks and channel characteristics. Although the method applies well to deck type bridges, there is no direct application for using the method when an arch bridge is used to make an indirect measurement.

In October, 1957, the Colorado State University in cooperation with the U.S. Bureau of Public Roads published a bulletin by H. K. Liu,[6] J. N. Bradley and E. J. Plate entitled "Backwater Effects of Piers and Abutments". A rigorous and extensive investigation of the backwater effects of piers and abutments has been given. The paper includes a complete analysis of the energy losses through the constriction. In the end, an approximate simple method of analysis is provided for the highway engineer to use. The general principle of the method is the conservation of energy. A number

of graphs based upon laboratory data were developed for determining the maximum backwater and the differential level of water surface across the embankment. This method was reproduced in a bulletin published by the Bureau of Public Roads[7] in October, 1958. Much of the work done at Colorado has been used as a comparison to the present research and reference to it will be made throughout this text.

H. R. Vallentine[8] reports on tests performed to study the characteristics of flow in a rectangular channel with symetrically placed, sharp edged constriction plates placed normal to the flow. The flow is related to the upstream depth by means of a weir type discharge equation. The experimental coefficients were found to depend upon the geometry of the constriction and the Froude Number of the unconstricted flow. The conditions which produce an increase in upstream depth were investigated and the extent of the increase evaluated.

Some recent work done at Lehigh University tells[9] about the effects of placing spur dikes on the upstream side of a bridge contraction. These dikes are designed to increase the hydraulic efficiency of the bridge crossing. The paper presents a good qualitative description of the energy loss through the contraction.

Husain[10] carried out a preliminary investigation upon which the present research is based. He studied both two and three dimensional semi-circular arch openings in a smooth flume. General centerline surface profiles were obtained and recommendations for future studies were made. A dimensional analysis of the problem was presented.

Soosky[11] developed, for the two dimensional case, both exact and approximate solutions of the discharge equation. He also continued the

small flume tests started by Husain. Included were two and three dimensional semicircular and two-dimensional segment tests in a smooth and rough channel. Several curves relating the backwater ratio to the normal depth Froude Number were presented for several arch diameters. A more detailed presentation of the results of these tests will be discussed in a later section. Much of Mr. Sooky's data has been reanalyzed to fit more recent techniques.

ANALYSIS:

Figure 1 shows a definition sketch of the effect of a channel constriction on the water surface profile. Section views B and C illustrate the two types of centerline surface profiles obtained with mild and steep slopes. The most generally occuring situation which appears in actual practice is idealized by section B. The depth y_o is at a point far enough upstream such that the flow is basically unaffected by the M_1 backwater curve. y_1 is the point of maximum backwater. y_2 is at the section of minimum jet area or the vena contracta. y_3 is the minimum water depth of the regain curve and y_4 is again at a point sufficiently downstream from the contraction where the flow returns to the normal depth.

For any physical problem such as this, a dimensional analysis is convenient for the purpose of guidance and interpretation of a testing program. In this manner the basic variables can be grouped into dimensionless quantities and their relationships investigated. In the problem at hand, it is desired to determine the maximum water depth upstream of the constriction. It is assumed that the variables which govern the backwater superelevation may be grouped into three catagories as follows: (The reader is asked to refer to Figure 1 for an illustration of the terminology.)

a.) For the fluid

ν, the absolute viscosity

ρ, density of the fluid

g, acceleration of gravity

b.) For the stream flow

y_1, maximum water depth upstream of constriction (section 1)

y_o, the normal depth of flow in the approach channel. (section o)

V_o, the velocity of flow at normal depth.

n, Manning's roughness coefficient of the approach channel.

Δh, the maximum water surface drop across the constriction.

c.) For the constriction

A_θ--The total normal depth flow area.

A_β--The flow representing that portion of the A that passes through the bridge without contraction.

Hence, from the above list of variables,

$$y_1 = f_1 (y_o, V_o, n, \Delta h, \nu, \rho, g, \theta, b) \quad (1)$$

Buckingham's theorum[12] states that in a physical problem including n quantities in which there are m dimensions, the quantities may be arranged into (n-m) dimensionless parameters. With the mass, length and time systems of units the n-m or seven dimensionless π parameters are as follows,

$$y_1/y_o = f_2 \left(y_o g/V_o^2, \nu/V_o y_o, n/y_o^{1/6}, A_\theta/y_o^2, A_\beta/y_o^2, \Delta h/y_o \right) \quad (2)$$

Inverting the first two parameters

$$y_1/y_o = f_3 \left(V_o^2/g y_o, V_o y_o/\nu, n/y_o^{1/6}, A_\theta/y_o^2, A_\beta/y_o^2, \Delta h/y_o \right) \quad (3)$$

In equation (3) the term $V_o^2/g y_o$ is equivalent to the square of the normal depth Froude Number. Also $V_o y_o/\nu$ is the Reynolds Number. It is well

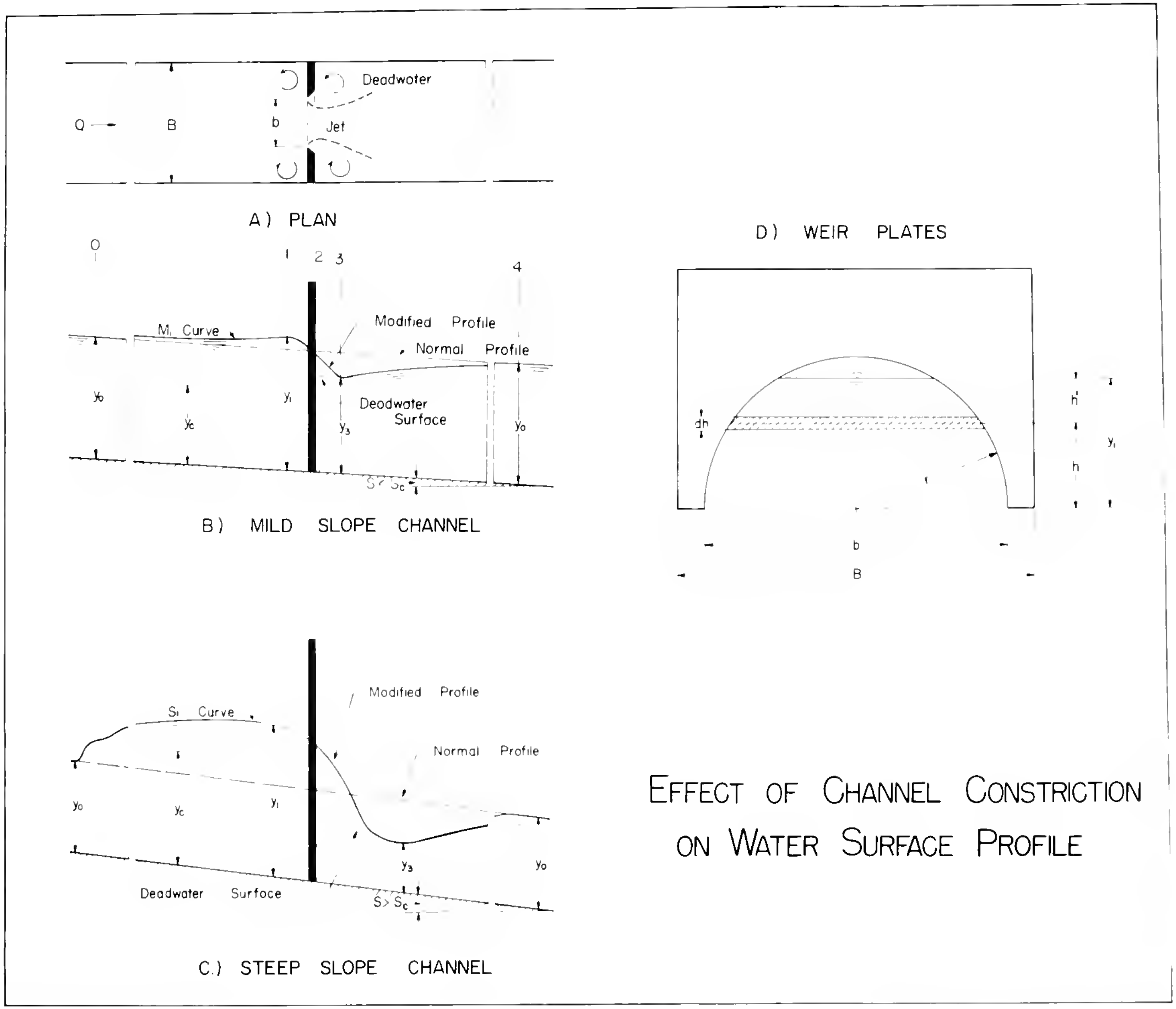
Q
B
b
Jet
Deadwater
A) PLAN
0
1
2
3
4
M_1 Curve
Modified Profile
Normal Profile
y_0
y_c
y_1
y_3
Deadwater Surface
$S < S_c$
B) MILD SLOPE CHANNEL
S_1 Curve
Modified Profile
Normal Profile
y_0
y_c
y_1
y_3
Deadwater Surface
$S > S_c$
C.) STEEP SLOPE CHANNEL
D) WEIR PLATES
dh
h'
h
y_1
b
B
EFFECT OF CHANNEL CONSTRICTION
ON WATER SURFACE PROFILE

Figure 1

known that gravity forces are predominant in open channel flow whereas viscous forces play a secondary rule. The Reynolds Number may therefore be disregarded for determining y_1/y_0. Furthermore, by assuming that the shape of the water surface downstream does not affect materially the shape of the water surface upstream, the term $\frac{\Delta h}{y_0}$ can also be eliminated. By combining the ratios $\frac{A_0}{y_0^2}$ and $\frac{A_g}{y_0^2}$ into $\frac{A_g}{A_Q}$ and excluding the above mentioned terms equation (3) becomes

$$y_1/y_0 = f_4\left(F_0^2, \; y_0^{1/6}/n, \; A_g/A_Q\right) \qquad (4)$$

The backwater ratio is therefore expected to be a function of the normal depth Froude Number, the channel roughness and the ratio A_g/A_Q.

The channel-contraction ratio (m') is defined in the present research as that portion of the total normal depth flow which can pass through the bridge waterway without contraction. By definition it is equivalent to the ratio A_g/A_Q obtained from the dimensional analysis. Along with the normal depth Froude Number, the contraction ratio is perhaps the most critical variable in the problem. As defined, the contraction ratio is a hypothetical term which owes its significance only to the geometry of the constriction.

Referring to figure 2, for the rectangular case, the total flow is that flow in area ADEH, and the flow that passes through the bridge opening without contraction is that represented by the area BCFG. Therefore the contraction ratio m' is

$$m' = q/Q \qquad (5)$$

If we assume that there is a constant uniform velocity V_0 across the whole normal depth section, equation (5) becomes

$$m' = q/Q = A_g V_0/A_Q V_0 = A_g/A_Q = b y_0/B y_0 = b/B \qquad (6)$$

However, for an arch bridge, as shown also in fig. 2, the surface width will be different for each and every normal depth y_o. Therefore in the same manner,

$$m' = q/Q = A_q V_o / A_Q V_o = A_q / A_Q \qquad (7)$$

The ratio of the two areas is clearly not equivalent to b/B. (For simplicity, b/B is hereafter defined by the symbol m.)

For that portion of a semi-circular arch with radius r and depth y_o the area becomes[18]

$$A_q = \int_0^{y_o} 2\sqrt{r^2 - y^2}\, dy = 2\left[\frac{1}{2}\left\{y_o\sqrt{r^2 - y_o^2} + r^2 \sin^{-1} y_o/r\right\}\right] \qquad (8)$$

The arch shown in figure 2b has a radius r and springline width b. The arch has been superimposed upon flow area of depth y_o. The center of curvature is at a distance d below the springline of the arch. The flow area (A_Q) of the rectangular channel is By_o, while the area representing that flow through the arch is given by

$$A_q = \int_0^{D} 2\sqrt{r^2 - y^2}\, dy - \int_0^{d} 2\sqrt{r^2 - y^2}\, dy \qquad (9)$$

Now, equation 7 becomes

$$m' = \frac{A_q}{A_Q} = \frac{D\sqrt{r^2 - D^2} + r^2 \sin^{-1} D/r}{By_o} - \frac{d\sqrt{r^2 - d^2} + r^2 \sin^{-1} d/r}{By_o} \qquad (10)$$

By algebraic manipulation, eq. (10) can be reduced to a form containing several dimensionless ratios. The result of this reduction is

$$m' = m\, C_m \qquad (11)$$

where

$m = b/B$

and

$$C_m = \frac{1}{2}\left[\left\{\frac{\sqrt{1-(\beta+\alpha)^2} + \frac{1}{(\beta+\alpha)}\sin^{-1}(\beta+\alpha)}{\frac{\alpha}{\beta+\alpha}\sqrt{1-\beta^2}}\right\} - \left\{\frac{\sqrt{1-\beta^2} + \frac{1}{\beta}\sin^{-1}\beta}{\frac{\alpha}{\beta}\sqrt{1-\beta^2}}\right\}\right] \qquad (12)$$

with

$\beta = d/r$

and

$\alpha = y_o/r$

In the form of equation (11) the value of m=b/B is adjusted for the particular arch by an amount equivalent to C_m such that m' is the same as the ratio of A_b to A_a. Kindsvater, Carter & Tracy[5] and Liu[6], as well as others have defined the contraction ratio as simply b/B or 1-b/B. In the more general case, equation (11) can be used for vertical abutment bridge piers as idealized in figure 2a by using a value of C_m of unity. Also, previous writers have stated that the contraction ratio is equivalent to a ratio of the conveyances in the contracted and uncontracted regions. The authors feel that, as defined, m' is more truly a ratio of areas rather than conveyances since the conveyance employs both the hydraulic radius and a roughness coefficient.

In the general case, the values of α and β can take on numbers within certain limits, before the normal depth will submerge the crown of the arch. The limits are as follows

For $\alpha = y_o/r$ $$\frac{0}{r} \leq \frac{y_o}{r} \leq \frac{r-d}{r} \qquad (13)$$

or

$$0 \leq \alpha \leq (1-\beta)$$

For $\beta = d/r$ $$0 \leq \beta \leq 1 \qquad (13a)$$

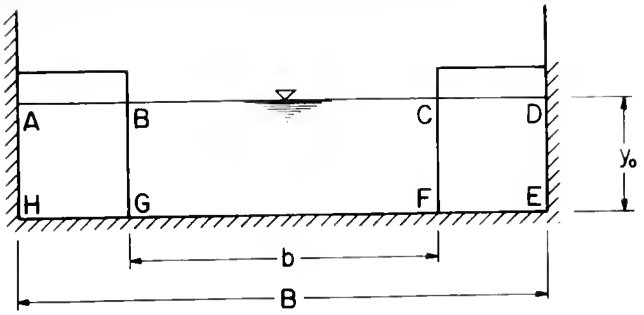

FLOW IN ADEH = $Q = V_o B y_o$

FLOW IN BCFG = $q = V_o b y_o$

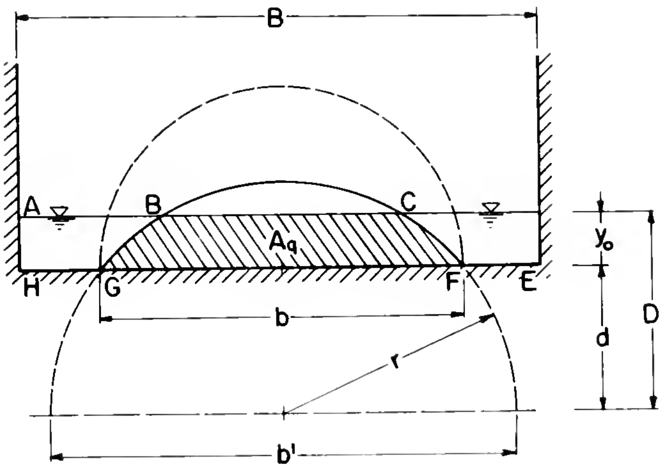

FLOW IN ADEH = $Q = V_o B y_o$

FLOW IN BCFG = $q = V_o b y_o$

DEFINITION SKETCH FOR THE DEVELOPMENT OF

THE CONTRACTION RATIO

Figure 2

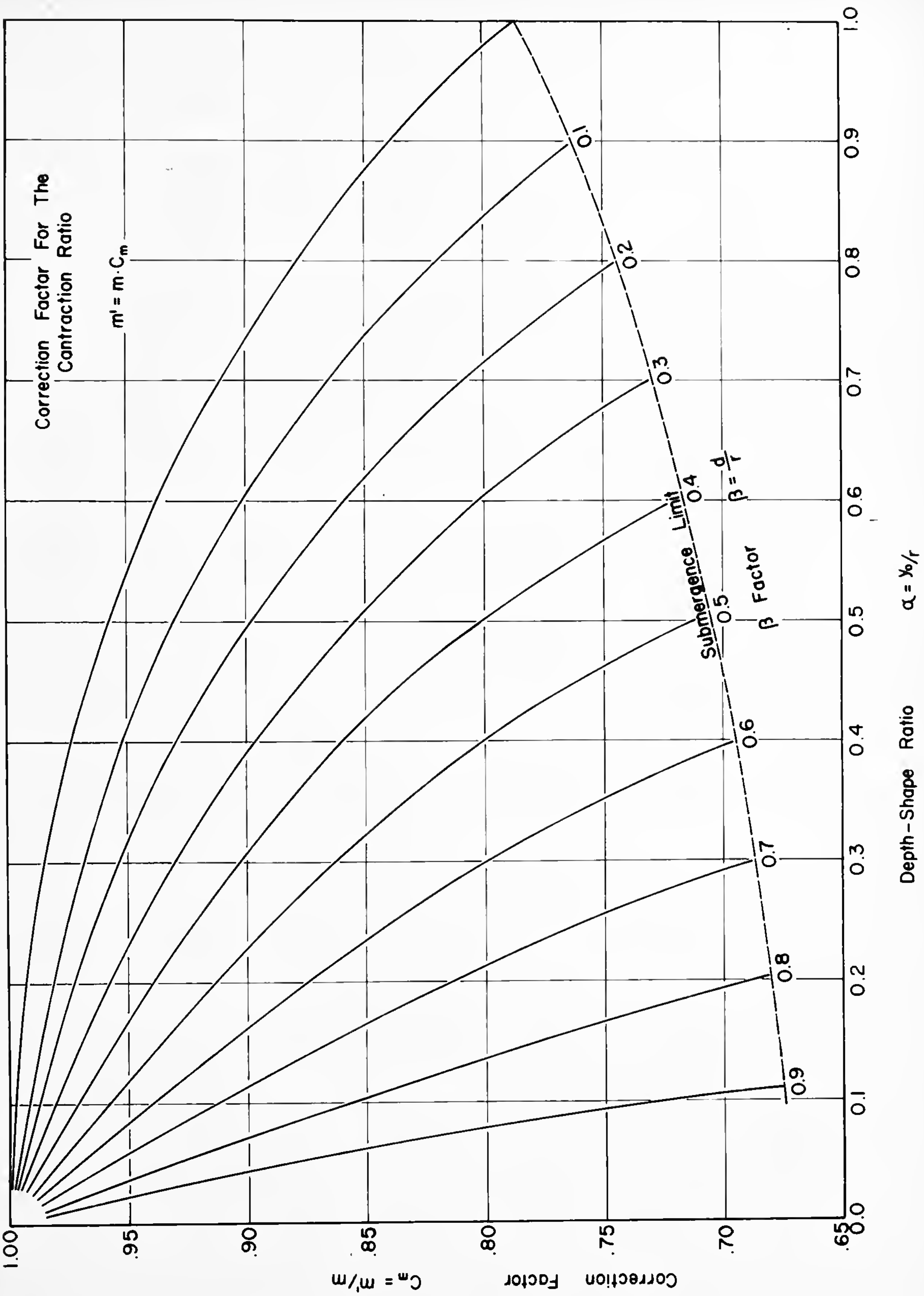
Correction Factor For The Contraction Ratio
m' = m·C_m
Submergence Limit
β = d/r
β Factor
0.1
0.2
0.3
0.4
0.5
0.6
0.7
0.8
0.9
Correction Factor C_m = m'/m
1.00
.95
.90
.85
.80
.75
.70
.65
Depth-Shape Ratio α = y₀/r
0.0
0.1
0.2
0.3
0.4
0.5
0.6
0.7
0.8
0.9
1.0

Figure 3

When $\beta = 0$, the case of a semi-circular arch with the center of curvature at the springline exists. When $\beta = 1$ the arch does not exist.

The values of m_m have been calculated for several α's and β's and are summarized in the graph of figure 3. The submergence limit represents the upper limits of both α and β. The segment arch which is a constant radius arch with its depth below the springline (i.e. $\beta > 0$) can be used as an arch in its own right or as an approximation to an elliptical or a multiple radius arch. The value of m' for the latter two cases could also be determined directly from eq. 7. However, they have not been worked out in the present research.

An approximate solution of the discharge equation in a rectangular channel with a sharp crested semi-circular constriction was obtained and is expressed in terms of an infinite series of powers of the ratio y_1/r. With reference to figure 4, the Bernoulli theorum gives:

$$Q = \int V\,dA = \int_0^{y_1} c\sqrt{2g(y_1 - h)} \cdot 2\sqrt{r^2 - h^2}\,dh \qquad (14)$$

Expanding equation (14) into a series and integrating term by term and making use of the fact that 2r=b:

$$Q = C_d\sqrt{2g}\,\frac{17}{24}\,y_1^{3/2}\,b\left[1 - 0.1294\left(\frac{y_1}{r}\right)^2 - 0.0177\left(\frac{y_1}{r}\right)^4 + \cdots\right] \qquad (15)$$

This may be written as

$$Q = c\,y_1^{3/2}\,b\,M \qquad (16)$$

where

$$c = C_d\,\frac{17}{24}\sqrt{2g} \qquad (17)$$

and

$$M = \left[1 - 0.1294\left(\frac{y_1}{r}\right)^2 - 0.0177\left(\frac{y_1}{r}\right)^4 + \cdots\right] \qquad (18)$$

The discharge in a rectangular flume may also be expressed by

$$Q = V_o A_o = \mathbb{F}_o \sqrt{g}\, B\, y_o^{3/2} \qquad (19)$$

where $$\mathbb{F}_o = V_o / \sqrt{g y_o}$$

is the Froude Number of the undisturbed normal depth flow. Equating (15) and (19) and solving for the coefficient of discharge

$$C_d = \frac{12\sqrt{2}}{17} \cdot \frac{\mathbb{F}_o}{m M}\left(\frac{y_o}{y_1}\right)^{3/2} \qquad (20)$$

Since $m = m'/C_m$ eq. 20 may be rearranged such that the backwater ratio becomes

$$\frac{y_1}{y_o} = \left[\frac{12\sqrt{2}}{17}\, \frac{\mathbb{F}_o\, C_m}{C_d\, m'\, M}\right]^{2/3} \qquad (21)$$

Typical values of the discharge coefficient Cd are shown in figure 15 which shows the results the two-dimensional semi-circular arch tests in the rough rectangular channel. It is interesting to note the limiting conditions of the discharge coefficient as m' goes from zero to one. For a two-dimensional ideal orifice, Streeter[16] shows that the application of complex variables to the "Schwarz-Christoffel Theorum" (better known as the theory of free streamlines) leads to an ideal discharge coefficient of

$$\frac{2b}{\frac{4b}{\pi} + 2b} = \frac{\pi}{\pi + 2} = .611 \qquad (22)$$

The coefficient of discharge curves of figure 15 seem to converge to .611 showing that this is a limiting value of Cd as m' approaches zero.

When m' is equal to unity, Cm=1 and b/B= 1. Therefore b... ...d there is no contraction at all. If there is no contraction, then y ... = ... and M = 1 . Also $\frac{12\sqrt{3}}{17}$ = .9981 which is approx. unity. Therefore eq. 21 becomes

at m'=1

$$1 = \left(\mathbb{F}_o / C_d \right)^{2/3} \tag{23}$$

$$\text{or} \qquad C_d = \mathbb{F}_o$$

This can also be seen in the graphs of the discharge coefficient vs the contraction ratio for the two-dimensional case.

It has been observed by the authors that the equations derived by several different investigators for the backwater ratio produced by various constriction geometry's seem to have a basic similarity. As an example, equation(21) in the present text for y_1/y_o appears to be some function of $\left(\mathbb{F}_o/m'\right)^{2/3}$. An equation for the backwater ratio given by Valentine[3] for lateral con striction plates is

$$y_1/y_o = \left(\frac{g \;\mathbb{F}_o}{C\,(1-m)} \right)^{2/3} = g_2\left(\frac{\mathbb{F}_o}{m'} \right)^{2/3} \tag{24}$$

$$\text{where} \qquad m = \frac{B-b}{B} = 1 - \frac{b}{B} = 1 - m' \qquad (C_m = 1)$$

Also Liu[6] presents an empirical formula for a two-dimensional vertical-board model

$$\left(\frac{h_1^*}{h_n} \right)^3 = 4.483\,\mathbb{F}_o^2 \left[\frac{1}{M^2} - \frac{2}{3}\left(2.5 - M\right) \right] + 1 \tag{25}$$

where $M = b/B = m'$ $(C_m = 1)$

Considering only the leading term $1/M^2$ in the quantity in bracket ( )

becomes

$$\frac{h_1^*}{h_n} = g_5\left(\frac{F_0}{m'}\right)^{2/3} \qquad (25a)$$

It appears that with the proper interpretation of the variables, namely m' & F_0, the results of tests performed on different geometric shapes of bridge openings should produce the same results. For instance, a vertical abutment deck-type bridge may physically appear completely different than a semi-circular arch bridge. However, hydraulically speaking if they have the same contraction ratio m', they should produce the same backwater ratio. The limitations of the assumption must necessarily lay in the fact that both bridges must have the same eccentricity, skewness and entrance conditions. It is believed that this concept applies equally as well to multiple span bridges. An attempt has been made to compare the two-dimensional semi-circular test results of the author the segment data obtained by Sooky, and the VB data as given by Liu.[6] The results of this comparison will be shown and discussed in a later section.

EXPERIMENTAL SET-UP:

A. Main Testing Facilities

For the purpose of preliminary testing, a small variable slope flume 6" wide and 12' long was built. The channel sides and bottom were constructed of lucite and carefully alligned by means of adjusting screws. The slope of the flume was contr lled by a hand operated scissor jack at the lower end of the flume. An aluminum I-beam mounted horizontally above

the flume served as a track for the mechanical and electric point gage used in obtaining the water surface measurements. The electric point gage consisted of two metal points that were hooked up to a set of batteries and a galvanometer. When the second metal point would make contact with the water surface, the circuit would close and the galvanometer would deflect. The flow was metered by a 1 inch orifice plate in a 2 inch supply line. Two and three dimensional tests were run in both a smooth and rough flume. For the rough tests, the walls were lined with copper wire mesh of 16 meshes per inch.

The majority of the tests reported here were performed in the larger 2 foot by 5 foot by 64 foot all steel tilting flume. The slope was controlled by six screw jacks that were designed and installed such that the rate of rise and fall of each jack per turn of a single drive shaft was proportional to the distance from the pivot point of the flume. The jacks were driven by a common motor and gear reducer. The motor was operated by a raise, lower and stop switch. A revolution counter was attached at one end of the drive shaft and the actual slope of the flume bed was related to the number of revolution and tenths of revolutions of the shaft. In this manner a change of slope with an accuracy of ± 0.0000025 feet/feet was easily accomplished in a matter of minutes. At the discharge end of the flume an adjustable sharp crested rectangular weir made of lucite was installed. A catchment box was made to eliminate any splash. The box discharged directly to the sump. An 8 foot by 10 foot head box was equipped with an elliptical transition to provide a smooth change as the water flowed into the flume. The head box also contained several screens and one large stone baffle. A skimming board

which floated on the water was installed at the flume entrance in order to eliminate surface waves. For a more complete description of the testing flume see reference 15.

The water was taken from a large recirculatory sump. One 2000 GPM pump and one 300 GPM pump fed the head box. The actual inflow was metered by 2 venturi's. A complete layout of the flume and the water supply system is shown in figure 4.

An aluminum instrument rack was mounted on adjustable stainless steel guide rails running the length of the flume. On the rack was mounted an electric point gage and a 1/2 inch Prandtl Tube. The staff of the point gage was marked in millimeters and was equipped with a vernier which read to a tenth of a millimeter. The Prandtl Tube was the type used normally for air. It was connected to an inverted U manometer which had a fluid of specific gravity .810. Two surveyors tapes were used to determine the location of a particular reading. One was installed lengthwise on the flume wall, and another transversally on the instrument rack. The rack along with the point gage and Prandtl Tube can be seen in figure 5a. In addition a 50-tube manometer stand was installed to obtain rapid measurements of the surface geometry. Fifty piezometer taps located at points along the centerline and 1 ft. and 2 ft. right and left of the centerline were hooked up to the manometer bank. The bank was constructed so that it could be tilted to a 45° angle and was illuminated from the inside. Figure 5b shows a picture of the completed manometer stand.

There were sixteen models used in the testing program. They were designed for specific values of b/B and L/b . For a relative length

ratio of L/b=0 four models were made: one for each of the following values of m=b/B, m=0.3, 0.5, 0.7, and 0.9. They were constructed with 1/2 inch marine plywood and faced with 22 gauge galvanized sheet metal. The three dimensional models were built with m values of 0.3, 0.5, 0.7, and 0.9. In each "m" group two models were constructed with L/b=0.25 and one model with L/b=0.5. The main construction was 1/2" marine plywood. The barrel was formed with galvanized sheet metal, and one side of one of the L/b=0.25 models was faced with lucite. Figure 6a illustrates the three-dimensional bridges. Shown are the four models with L/b=0.25 and m=0.3, 0.5, 0.7, and 0.9. The book and hammer are included to show perspective. With this combination of models we were able to test each of the openings m=0.3, 0.5, 0.7, and 0.9 for relative lengths L/b of 0, 0.25, 0.50, 0.75, and 1.00.

B. Boundary Roughness Analysis

The actual tests to determine the maximum backwater, were run under two different boundary roughnesses. The first roughness, which will be called the smooth boundary, consisted of the steel walls of the flume. The walls were finished with an epoxy resin paint. It was determined that the smooth flume produced a Mannings n value of .0110. This value was not representative of any natural physical condition. It was decided to run a second series of tests in a boundary roughness which would simulate a more natural condition. Assuming a scale of 1/10 between model and prototype, a Mannings n between 0.02 and 0.03 in the flume would have been desirable. This would correspond to field values of approximately 0.03 to 0.05 respectively. The flume was lined with a series of 1/4 inch aluminum rods. Two layers of rods were placed on the bed of the flume:

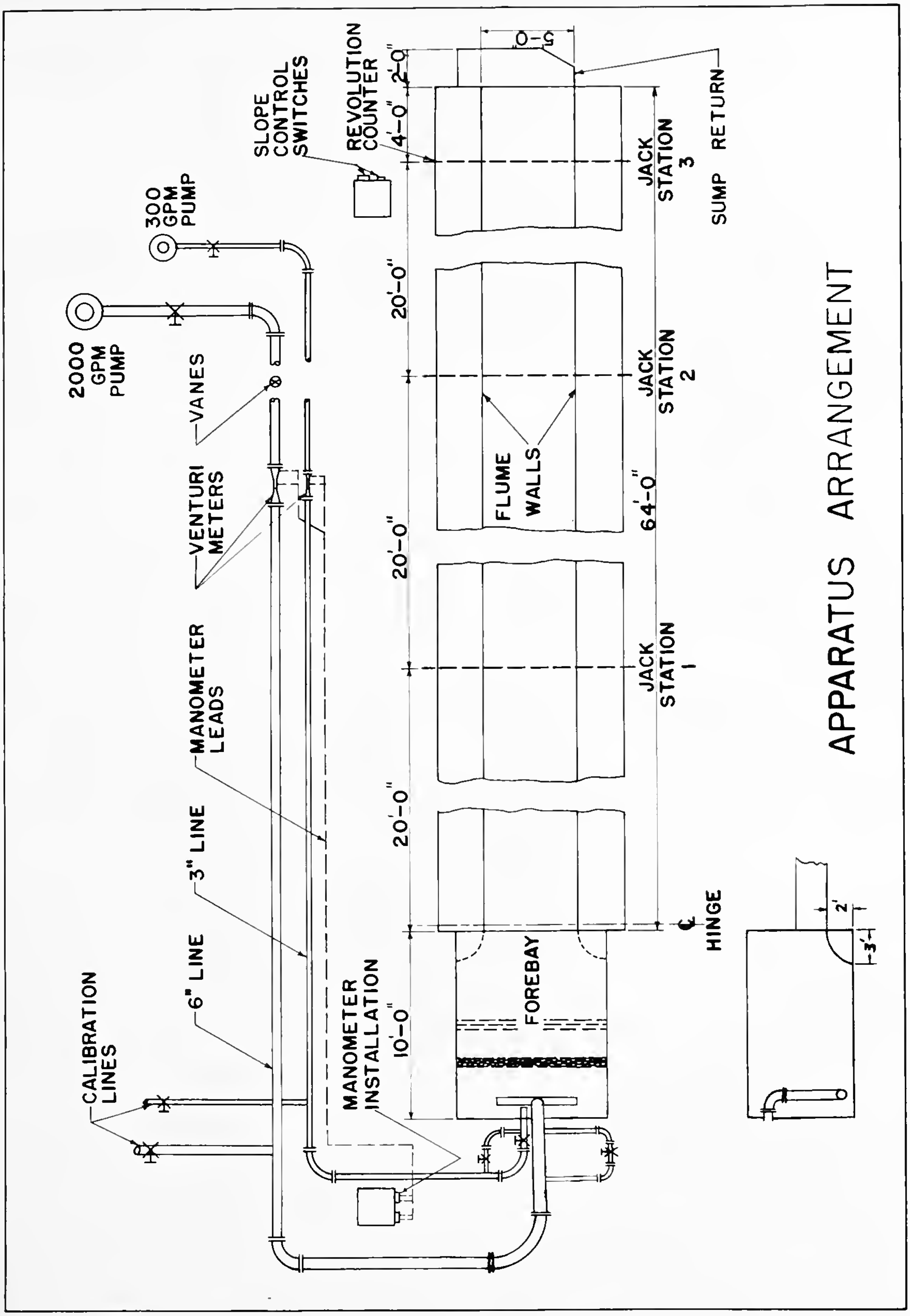

APPARATUS ARRANGEMENT

FIGURE 4

Figure 5a) Instrument Rack

Figure 5b) Manometer Bank

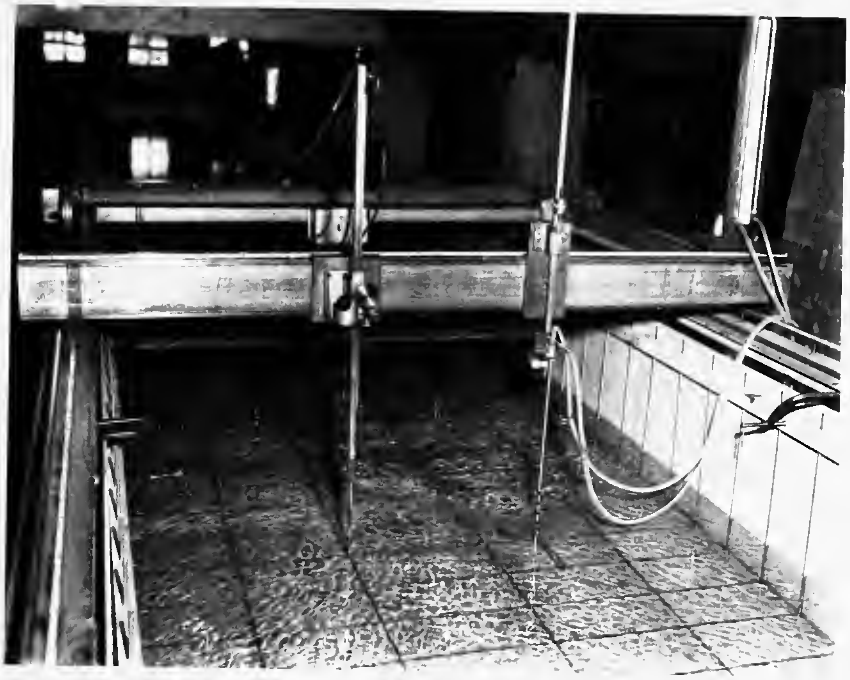

[illegible]

Figure 5b) Flume with Roughness Bars

a bottom layer of longitudinal bars placed 12 inches on center and a top layer of transverse bars 6 in. on center. Along the side wall, there was one layer of vertical bars 6 in. on center placed 1/4 in. from the wall. The bottom bars were tied together. The vertical bars were tied at the bottom and to the transverse bars and were clamped to the walls above the free surface. This roughness pattern is shown in figure 6b. After a series of normal depth test runs were made, it was found that this particular pattern gave a Manning's n of 0.0238. It was also found that steeper slopes and greater depths could be used without going out of the test range.

In order to test the consistency of the uniform flow depths for a given slope and flow, comparisons to several well known experimental results were made. The Darcy-Weisbach friction factor and the Reynolds Number for each uniform flow condition was caculated. For the "smooth" tests, the experimental friction factors were compared to the theoretical values obtained by adapting the Blasius and Prandtl-Von Karman formulas for flow in smooth pipes to the rectangular open channel. Figure 7 shows a plot of the Darcy Weisbach friction factor vs. the Reynolds Number for both the smooth and rough test data. The rough data has been broken down according to constant flow lines and constant hydraulic radius lines.

Sayre and Albertson[16] have presented a compreshensive report of the effect of roughness elements in rigid open channels. They state that a roughness parameter χ (chi) which depends "on the size, shape and spacing of the roughness elements", should completely describe the boundary roughness. The true value of χ depends on whether or not 1) the boundary is hydrodynamically rough-- negligible viscous effects, and 2) the channel is sufficiently wide such that any appreciable side wall effects are essentially eliminated. The general

resistance formula for rough flow given by Sayre and Albertson is

$$\frac{C}{\sqrt{g}} = 6.06 \log y_0/\chi \qquad 6)$$

According to the method they have described for determining the value of χ, the pattern of 1/4 inch aluminum rods used in this research gave a χ value of .0126. The value of 6.06 agrees very well with the present work. Figure 8 shows a graph of the roughness function($C/\sqrt{g}$) vs. the relative roughness y_0/χ for some of the rough normal depth data.

Several velocity profiles were taken at a condition of maximum slope and maximum flow. With the value of χ and the shear velocity defined as $\sqrt{\tau_0/\rho} = \sqrt{g\ y_0\ S}$ a dimensionless velocity profile was drawn. The equation describing this profile is

$$\frac{V}{\sqrt{\tau_0/\rho}} = 5.06 \log_{10} y/\chi + 4.6 \qquad (7)$$

Figure 9 shows the graph of this equation and compares it to the similar one defined by Sayre.[16] The difference in the constant may be due to the intense wall effects which were present.

Figure 10 shows a general resistance diagram for open channel flow. It is similar in nature to the famous Moody diagram for pipe flow. The curves that are plotted are those suggested by Sayre.[16] The smooth and rough test values have been plotted for comparison.

PRELIMINARY TESTING:

Several preliminary tests were run in the small 6" by 12' flume. The results of the two dimensional weir tests were put in graphical form by plotting the coefficient of discharge vs. the contraction ratio m" with the

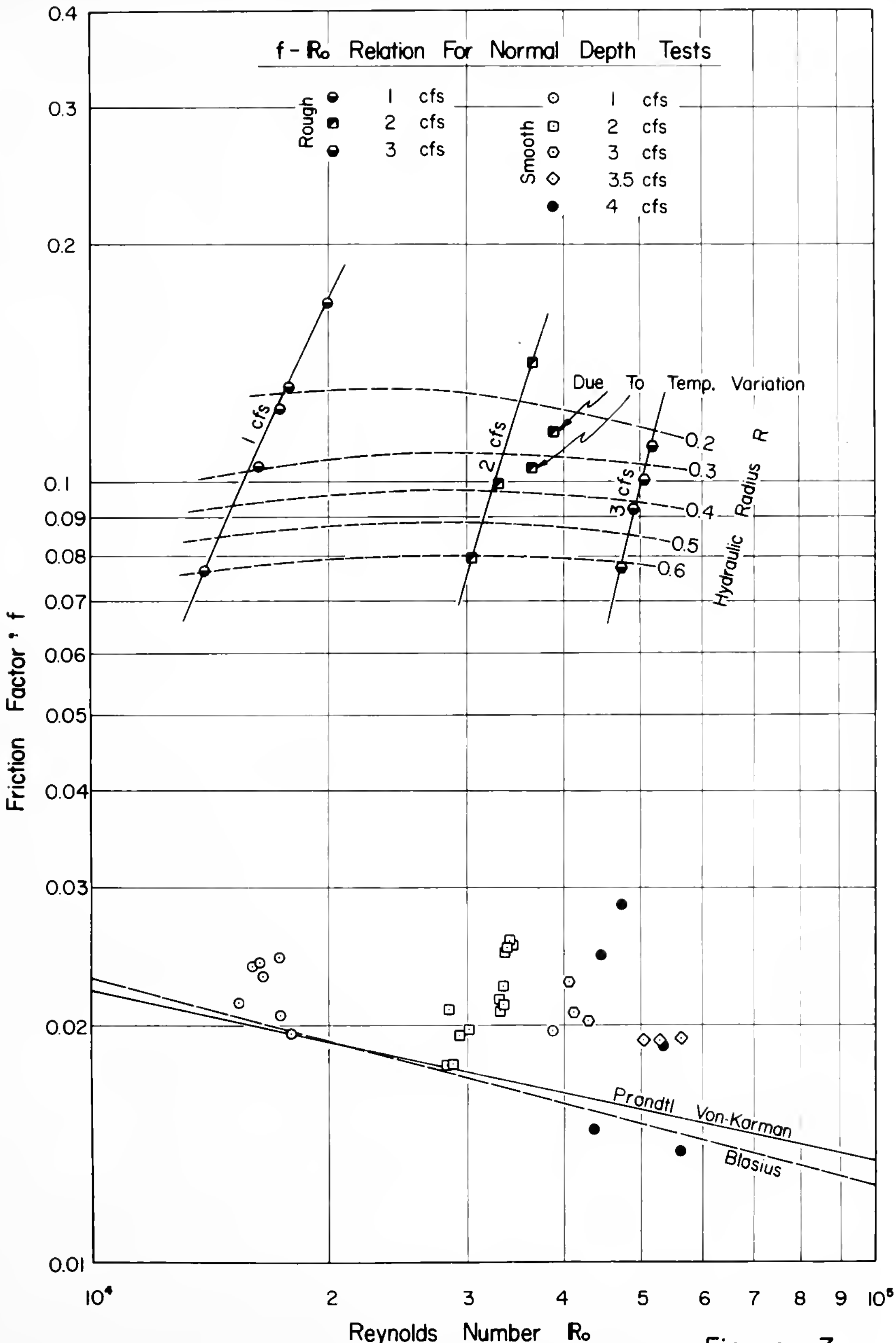
f - R₀ Relation For Normal Depth Tests
Rough
1 cfs
2 cfs
3 cfs
Smooth
1 cfs
2 cfs
3 cfs
3.5 cfs
4 cfs
Due To Temp. Variation
1 cfs
2 cfs
3 cfs
0.2
0.3
0.4
0.5
0.6
Hydraulic Radius R
Prandtl Von-Karman
Blasius
Friction Factor, f
0.4
0.3
0.2
0.1
0.09
0.08
0.07
0.06
0.05
0.04
0.03
0.02
0.01
10⁴
2
3
4
5
6
7
8
9
10⁵
Reynolds Number R₀

Figure 7

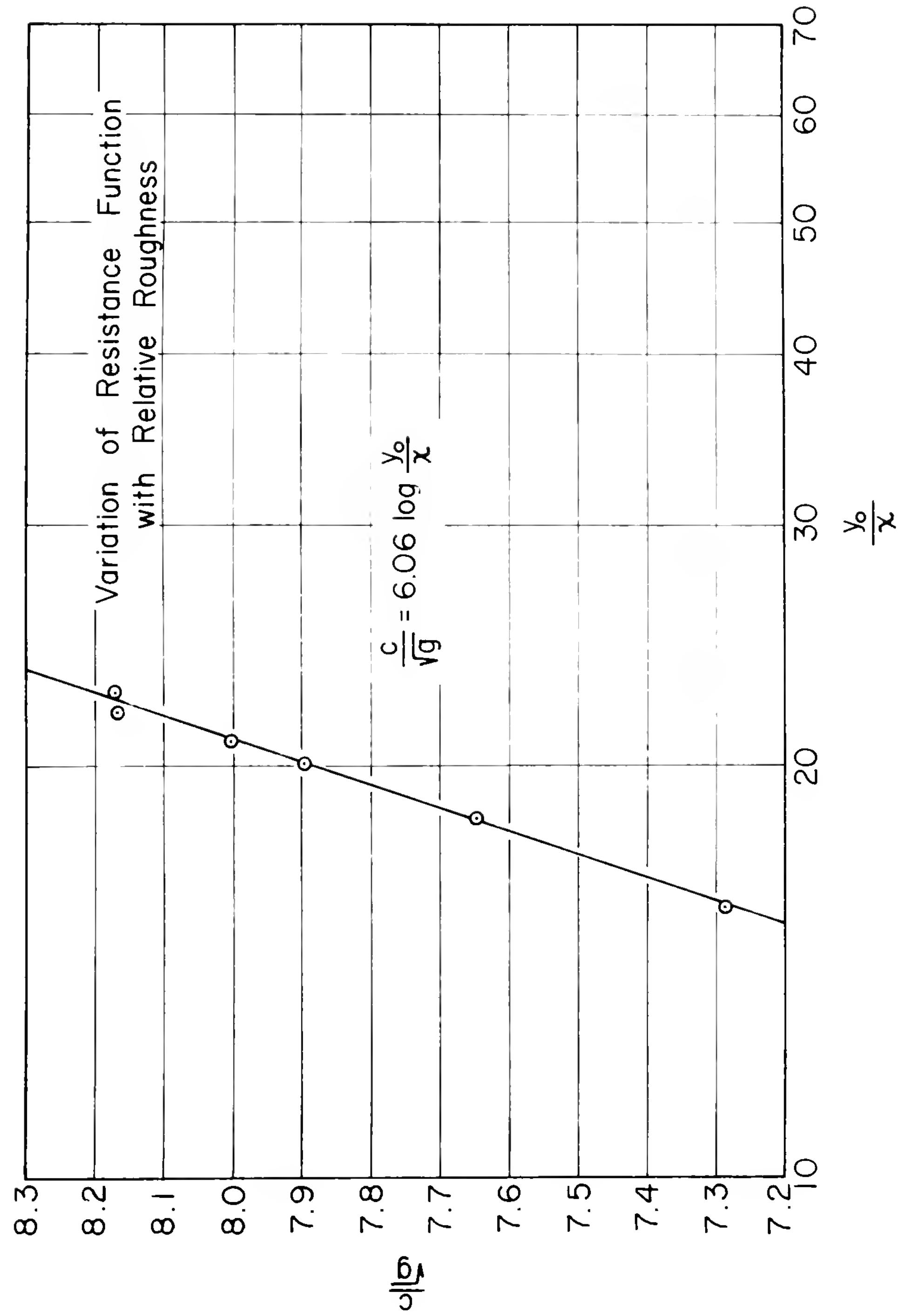
Variation of Resistance Function
with Relative Roughness
$\frac{c}{\sqrt{g}} = 6.06 \log \frac{y_o}{x}$
$\frac{c}{\sqrt{g}}$
8.3
8.2
8.1
8.0
7.9
7.8
7.7
7.6
7.5
7.4
7.3
7.2
10
20
30
40
50
60
70
$\frac{y_o}{x}$

Figure 8

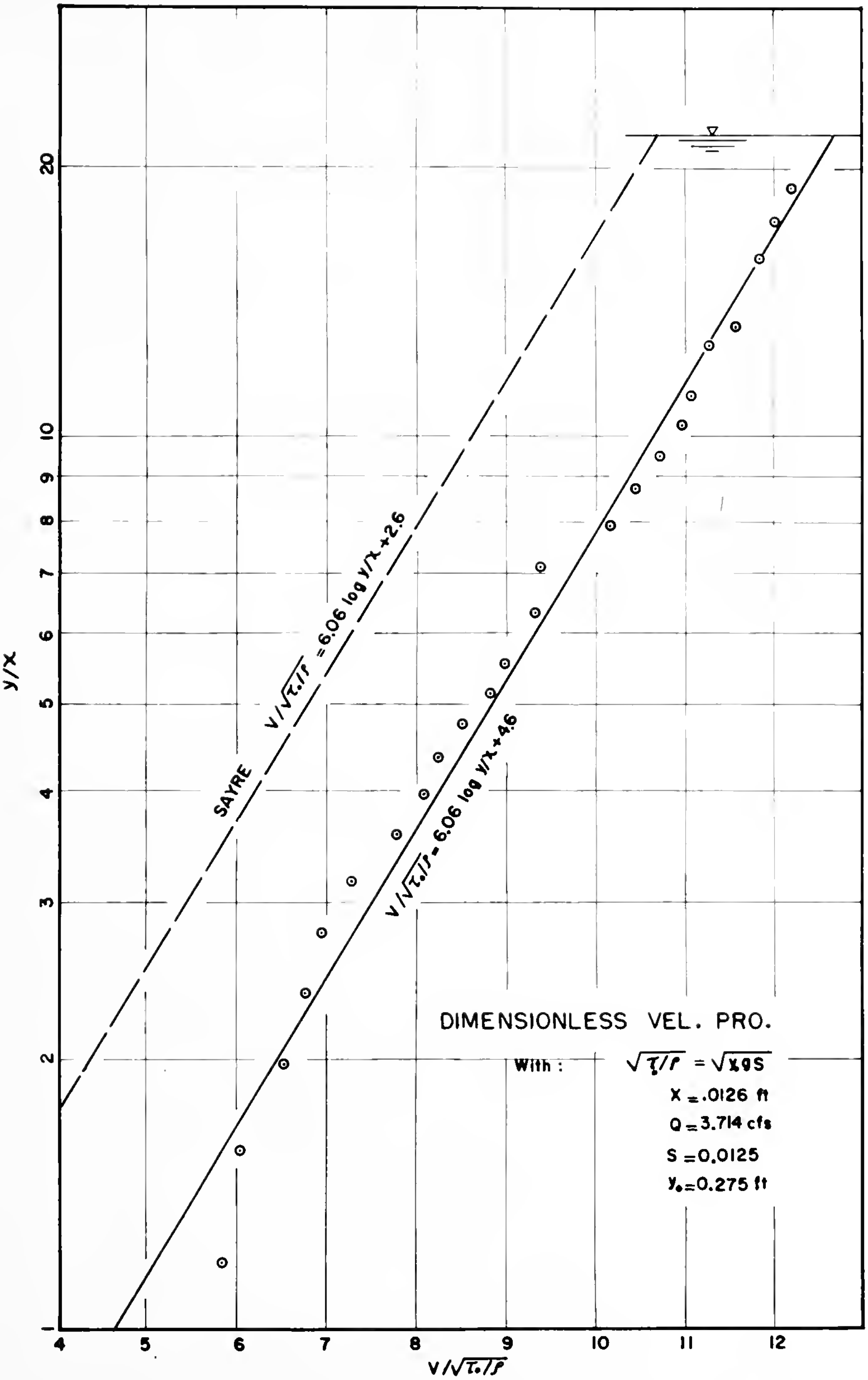
SAYRE
$V/\sqrt{\tau_o/\rho} = 6.06 \log y/\chi + 2.6$
$V/\sqrt{\tau_o/\rho} = 6.06 \log y/\chi + 4.6$
DIMENSIONLESS VEL. PRO.
With : $\sqrt{\tau_o/\rho} = \sqrt{\chi g S}$
$\chi = .0126$ ft
$Q = 3.714$ cfs
$S = 0.0125$
$y_o = 0.275$ ft
y/χ
$V/\sqrt{\tau_o/\rho}$

Figure 9

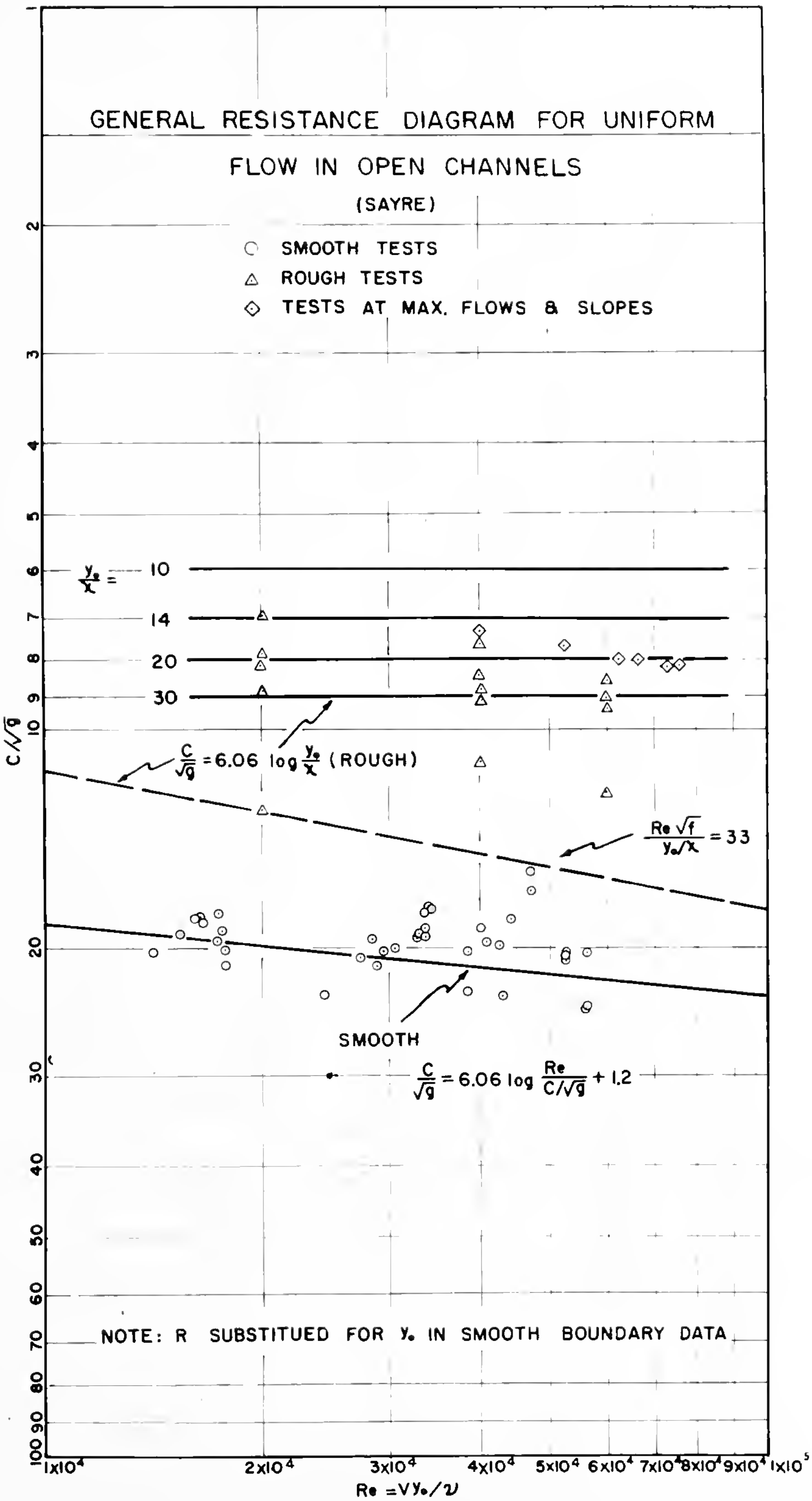
GENERAL RESISTANCE DIAGRAM FOR UNIFORM FLOW IN OPEN CHANNELS
(SAYRE)
○ SMOOTH TESTS
△ ROUGH TESTS
◇ TESTS AT MAX. FLOWS & SLOPES
$\frac{y_o}{x}$ = 10
14
20
30
$\frac{C}{\sqrt{g}} = 6.06 \log \frac{y_o}{x}$ (ROUGH)
$\frac{Re\sqrt{f}}{y_o/x} = 33$
SMOOTH
$\frac{C}{\sqrt{g}} = 6.06 \log \frac{Re}{C/\sqrt{g}} + 1.2$
NOTE: R SUBSTITUED FOR y_o IN SMOOTH BOUNDARY DATA
$C/\sqrt{g}$
2
3
4
5
6
7
8
9
10
20
30
40
50
60
70
80
90
100
1x10⁴
2x10⁴
3x10⁴
4x10⁴
5x10⁴
6x10⁴
7x10⁴
8x10⁴
9x10⁴
1x10⁵
$Re = Vy_o/\nu$

Figure 10

Froude Number F_o as a parameter. In addition, the relationship between F_o and y_1/y_o was plotted in a similar manner. (i.e. m' as the variable and F_o as the parameter).

The two-dimensional case was extended to the three-dimensional case by using semi-circular arch bridge models of the same b/B ratio and model length L of 24 inches. A comparison of the two and three-dimensional tests are compared in figure 11. It is interesting to note that at Froude Numbers less than 0.5 the effect of length was almost negligible. However at higher Froude Numbers the three-dimensional tests exhibited a smaller value of Cd and a larger backwater ratio .

The two-dim. semicircular-rough tests were analyzed and plotted. When the corresponding smooth tests were compared, the differences were found to be negligible. This indicated that the boundary roughness was not an influencing parameter at Froude Numbers less than 0.5. It was possible that the small scale effects due to increased surface tension could result in such a misleading conclusion. It was therefore necessary to verify this conclusion on a larger scale.

EXPERIMENTAL PROCEDURE:

When the smooth flume tests were started, the procedure was to arbitrarily select a slope and a flow, and then adjust the tailgate until a satisfactory normal depth was obtained. This proved to be a very tedious and unsatisfactory method. Before the rough testing was begun, an effort was made to determine an exact relationship between the several different variables required to produce a normal depth profile. A series of 24 different normal depth tests were run.

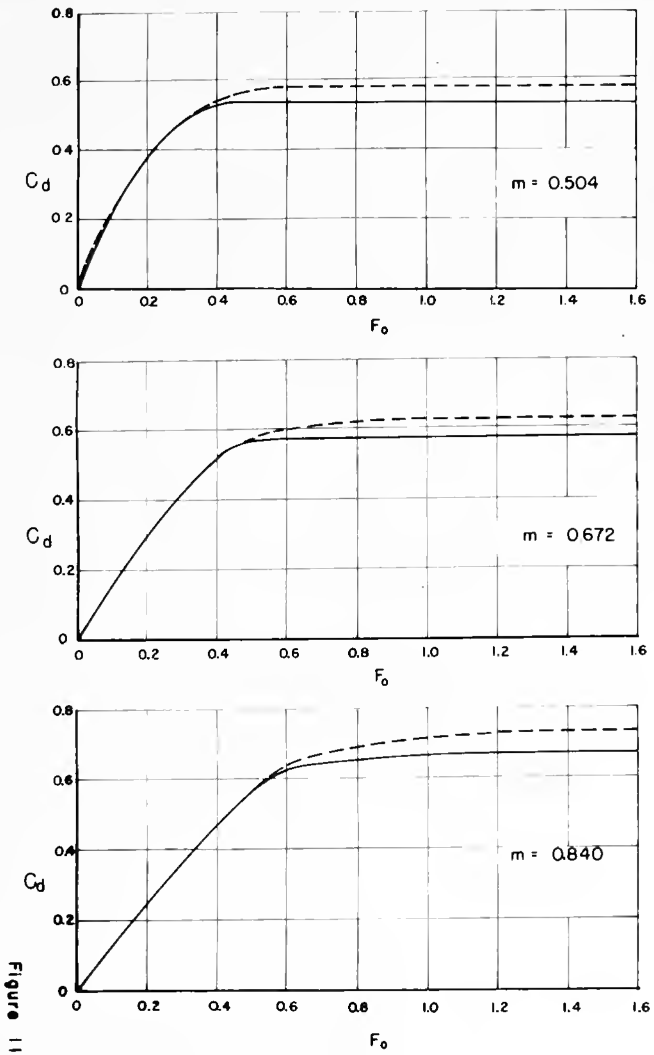

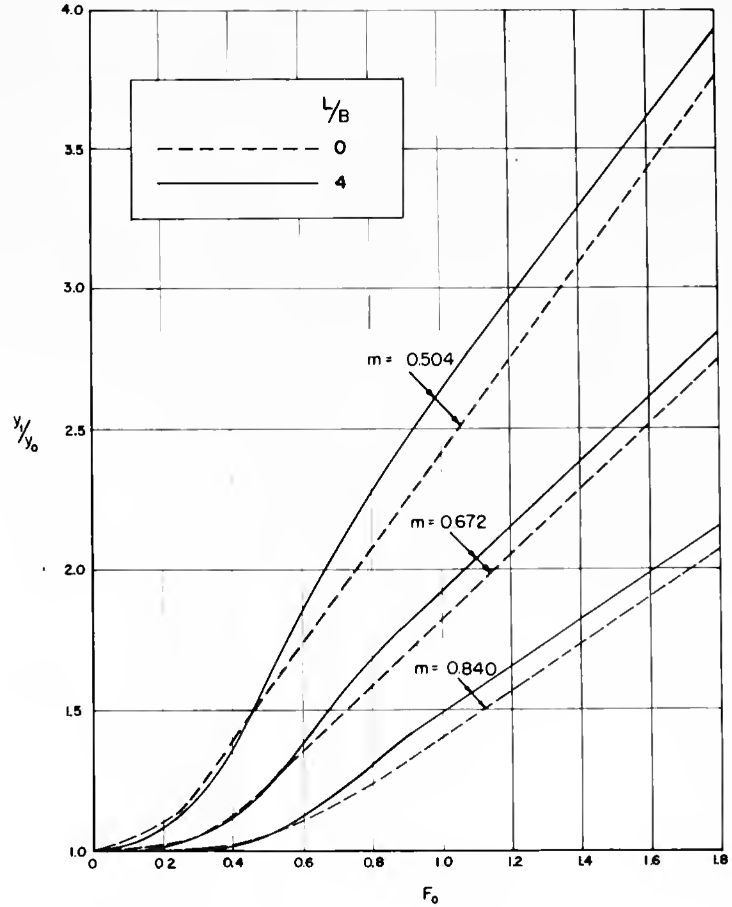

Figure 11

FLOW IN RECTANGULAR CHANNELS WITH SEMI-CIRCULAR CONSTRICTIONS - COMPARISON OF TWO AND THREE DIMENSIONAL CASES

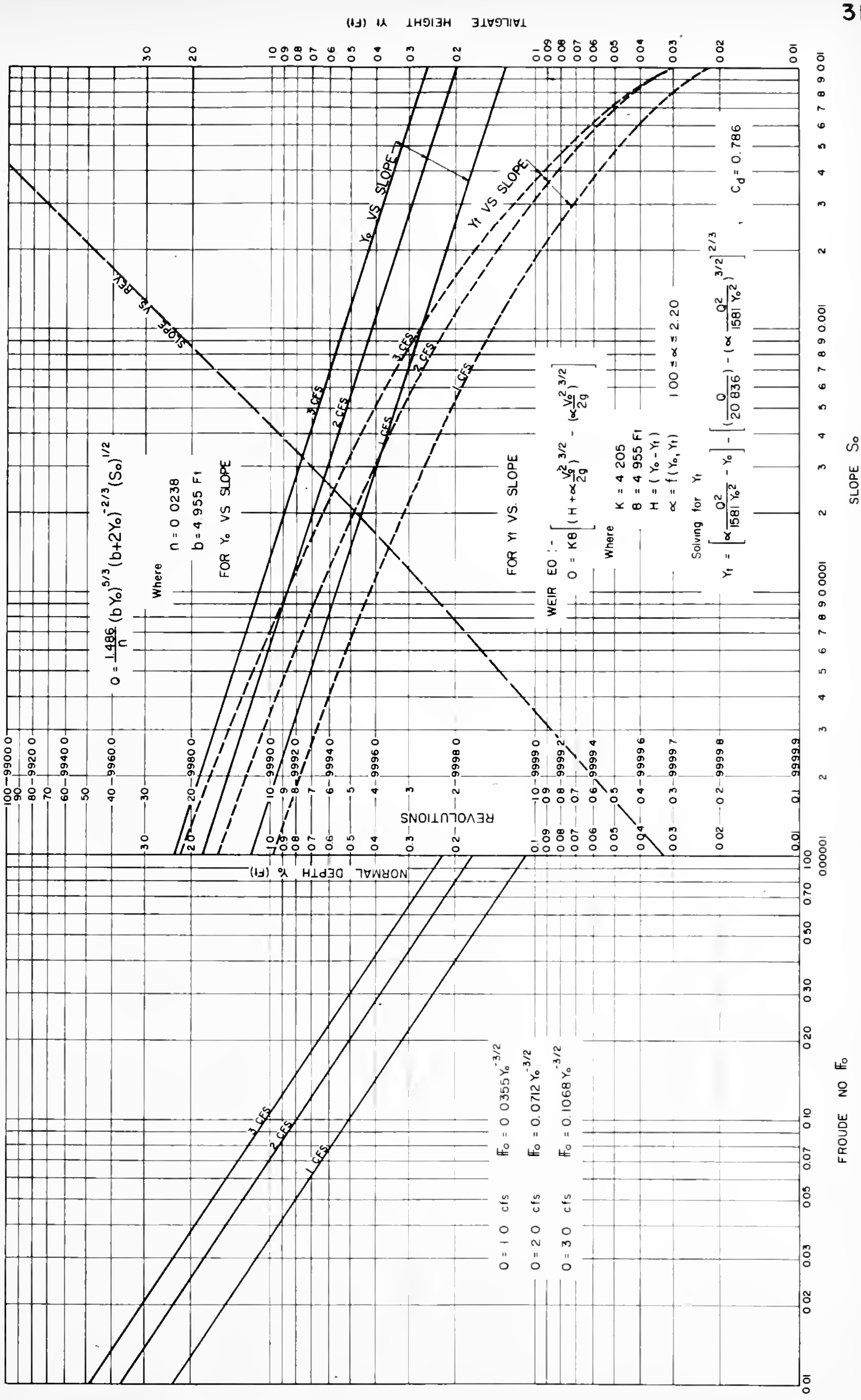
TAILGATE HEIGHT Yt (Ft)
NORMAL DEPTH Yo (Ft)
REVOLUTIONS
SLOPE So
FROUDE NO Fo
Yo VS SLOPE
Yt VS SLOPE
SLOPE VS REV
3 CFS
2 CFS
1 CFS
Q = 1.486/n (bYo)^5/3 (b+2Yo)^-2/3 (So)^1/2
Where
n = 0.0238
b = 4.955 Ft
FOR Yo VS SLOPE
FOR Yt VS. SLOPE
WEIR EQ :-
Where
K = 4.205
B = 4.955 Ft
H = (Yo - Yt)
α = f(Yo, Yt)
1.00 ≤ α ≤ 2.20
Solving for Yt
Cd = 0.786
Q = 1.0 cfs Fo = 0.0355 Yo^-3/2
Q = 2.0 cfs Fo = 0.0712 Yo^-3/2
Q = 3.0 cfs Fo = 0.1068 Yo^-3/2

FIGURE 12

From these preliminary tests, an average value of Mannings n of 0.0238 was computed. A calibration chart for selecting normal depths was made. This calibration chart is shown in figure 12. By using these curves to predetermine the slope, tail-gate-setting and normal depth to give a desired Froude Number at a given discharge, a vast amount of time-consuming work was eliminated. This method was used throughout the series of rough tests and proved to be very satisfactory. Only a few minor adjustments were needed.

The test procedure consisted of presetting the flow, slope and tailgate and then testing the various b/B and L/b models at these normal depth conditions. All depths were measured relative to the flume bottom. Depths were read along the centerline until the maximum upstream point had been reached and passed. Measurements were then taken along the downstream centerline until the minimum point had been reached and passed. This procedure was used for 95 smooth tests and 180 rough tests. A more extensive study of the surface topography and velocity profiles were performed on a few runs.

TESTS AND RESULTS:

A. Smooth Boundary Tests

The experimental values of y_1/y_0 for semi-circular constrictions in a smooth rectangular channel were plotted vs. the contraction ratio m and is shown in figure 13a. In a similar manner, the discharge coefficient Cd for the smooth flume tests is shown in figure 13b. The equation used to calculate this Cd is shown in the figure.

Since the smooth tests included only the results of the two dimensional models, it was needed to investigate further the effects of length as well as roughness in the rough tests. In order to test at low Froude

Numbers a very mild slope was required. Due to the smooth walls, it was difficult to obtain stable flow. The expanding flow at the downstream side of the construction was often unstable. It would deflect to one side or the other and would seldom remain evenly distributed. These testing difficulties were probably the cause for the scatter of smooth flow data points about the curve of the friction factor vs. the Reynolds Number in figure 7.

B. Rough Boundary Tests

The table below shows the conditions which were tested in the rough channel. The X's indicate the desired normal depth conditions in which the following values of m and L/b ratios were tested:

$$m = b/B = 0.3,\ 0.5,\ 0.7,\ 0.9$$

$$L/b = 0,\ 0.5,\ 1.0$$

The experimental conditions were obtained from the calibration chart of figure 12.

Flow Rate	Froude No.													
	.05	.10	.15	.20	.25	.30	.35	.40	.45	.50	.60	.70	.80	.90
1 cfs	X			X			X			X			[illegible]	
2 cfs		X			X			X			X			X
3 cfs			X			X			X			X		

The particular measurements that were taken on each of the above mentioned tests were those required to calculate the following quantities: The hydraulic radius, the Reynolds No. $\mathbb{R}_e$, the Froude No. $\mathbb{F}_o$, the friction coefficient f, the contraction ratio m', the discharge coefficient C_d, the backwater ratio y_1/y_o, the backwater superelevation h_1^*, the surface profile ratio $h_1^*/\Delta h$, the length to the maximum backwater elevation L_1, the length to the point of minimum depth L_3, $L_1 + L_3$, and Manning's n.

In view of the large amount of data that was to be analyzed and the repetitive character of the calculations, a program was prepared for processing the data on the Royal McBee LGP-30 digital computer. The total computer time required to calculate all of the above mentioned quantities for the 180 rough test runs was a little under nine hours. Without the computer, the time required for processing the data would have been prohibitive.

The backwater ratio y_1/y_c is shown in figure 14 for the semi-circular constrictions (L/b=0) in the rough channel. This plot is similar to that shown for the smooth channel in figure 13a. The graph clearly shows that as m' approached unity y_1/y_c goes to one. Also as m' goes to zero the backwater ratio approaches infinity. The actual test values are not shown since the curves of constant Froude Numbers have been graphically interpolated. The amount of error produced during the interpolating process was found in most cases to be less than one per cent. Similar plots have been made for the relative lengths L/b of 0.5 and 1.0.

A comparison of all of the L/b plots for backwater ratio has been made in figure 16a. These curves were produced by taking cross sections at m' values of 0.3, 0.5, and 0.7 from the plots of y_1/y_c vs. m'. It appears that the Froude No. and the contraction ratio are the governing parameters. Especially at lower Froude Numbers (below 0.5), the influence of the bridge length seemed to be small. The effect seemed to increase with a decrease in the contraction ratio. In the case of a small m', the physical proportions of the constriction are closer to those of a culvert rather than a bridge opening.

Figure 15 shows the graph of the discharge coefficient vs. the contraction ratio with the Froude Number F_o as a parameter for the

semi-circular rough tests. These curves were also interpolated for constant Froude Number lines. Similar graphs were drawn for the tests performed on the other three-dimensional models. The hump that appears in the Froude Number lines of 0.25 to 0.60 was a phenomena which appeared in all of the plots of the rough tests. A comparison of the several length ratios was also done by taking cross-section at constant m' values. A typical cross-section at m' = 0.7 is shown in figure 16b. This graph as well as other similar ones strongly reveals the fact that the bridge length is relatively unimportant and can for all practical purposes be disregarded.

In figure 17 the results of both smooth and rough tests are compared by the method of cross-sections. These curves verify the conclusion made from the small flume tests, that below a Froude Number of 0.5 the backwater produced by a given constriction is essentially the same for smooth and rough boundaries.

In order to completely describe the centerline profile it is desirable to have an estimate of the distance from the upstream face of the constriction to the point of maximum backwater elevation. This distance is referred to as L_1. Because of the flatness of the surface profile in the vicinity of the maximum point, it was extremely difficult to get an exact measurement of L_1. The actual measurements taken could have been in error by as much as $\pm$ 0.5 feet. However, with the large amount of data which was available, it was possible to study L_1 on an average basis. Average values of L_1 were calculated for several combinations of b/B, L/b, L/B, etc. In this manner, it appeared that the variable bridge length and the change in m' were of the same order of magnitude as the experimental error. The most consistent relationship was found by plotting the dimensionless

ratio L_1/b vs. the Froude No. with m=b/B as the parameter. This relationship is shown in figure 18a. The values of L_1 obtained from the sm... tests also compared favorably with figure 18a. In a similar manner it was found that the length L_1+L_3 (distance from the maximum point to the minimum point) varied only with the constriction geometry. The average values of L_1+L_3/b are plotted vs. m = b/B with L/b as a parameter in figure 18b.

Several other investigators have used the Froude Number at section 3 (see figure 1) as an estimator of the maximum backwater. Others have used F_3 as a controlling parameter in making indirect measurement of flood discharges. Due to the extremely irregular flow pattern at the minimum point it would seem that the use of F_3 may be very misleading. In the present research, the normal depth Froude No. F_0 was found to be a very reliable estimator of y_1/y_0. In order to test the variability of F_3 with F_0 a correlation curve of F_3/F_0 vs. F_0 was prepared. This curve is shown in figure 19. Below a Froude Number of 0.5 the correlation was good. However, above F_0 =0.5 the depth y_3 was often below the critical depth and the correlation of F_3/F_0 to F_0 was very poor. The scatter seemed to increase with increasing values of L/b. Therefore only the test results of the L/b=0 tests are shown. If used with caution these curves can be used to estimate the minimum depth y_3. It appears from this curve that F_0 is a much more reliable estimator than F_3.

C. Segment Analysis and Comparisions

With the introduction of m", the assumption was made that if properly interpreted the backwater produced by constrictions of the same m" would be equal regardless of the physical geometry of the actual constriction. In order to varify this assumption test data on constriction geometries other than a semi-circle was needed. A series of 50 tests were run

Smooth Test Results

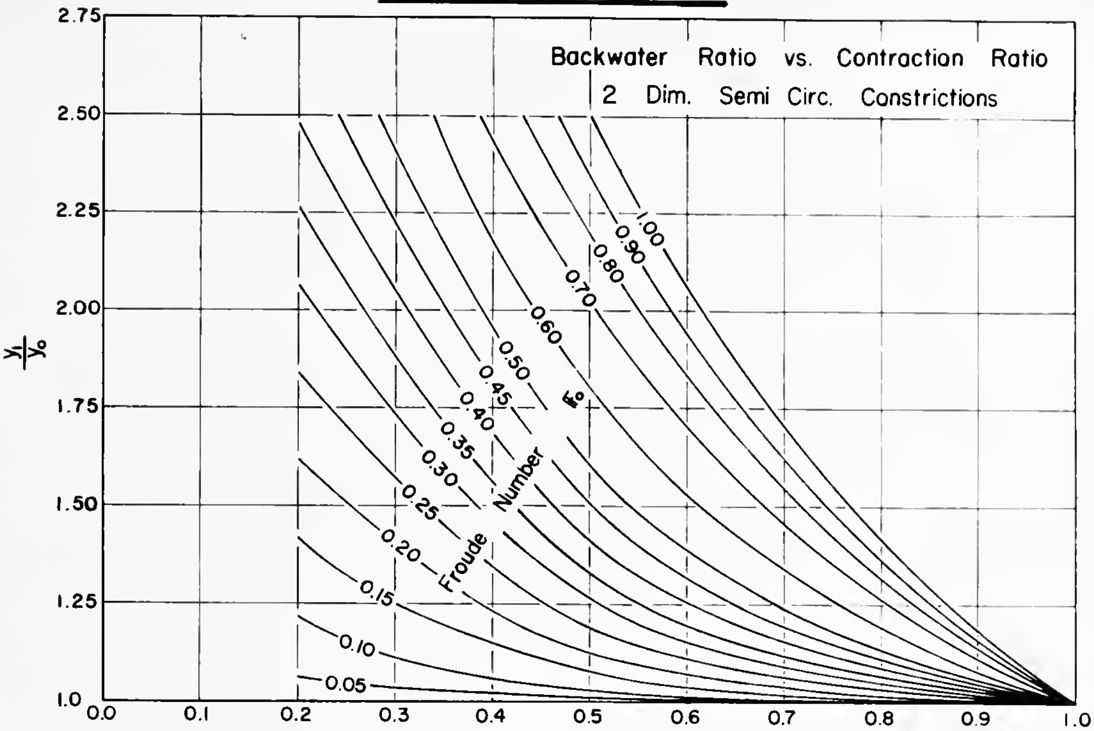

Figure 13a

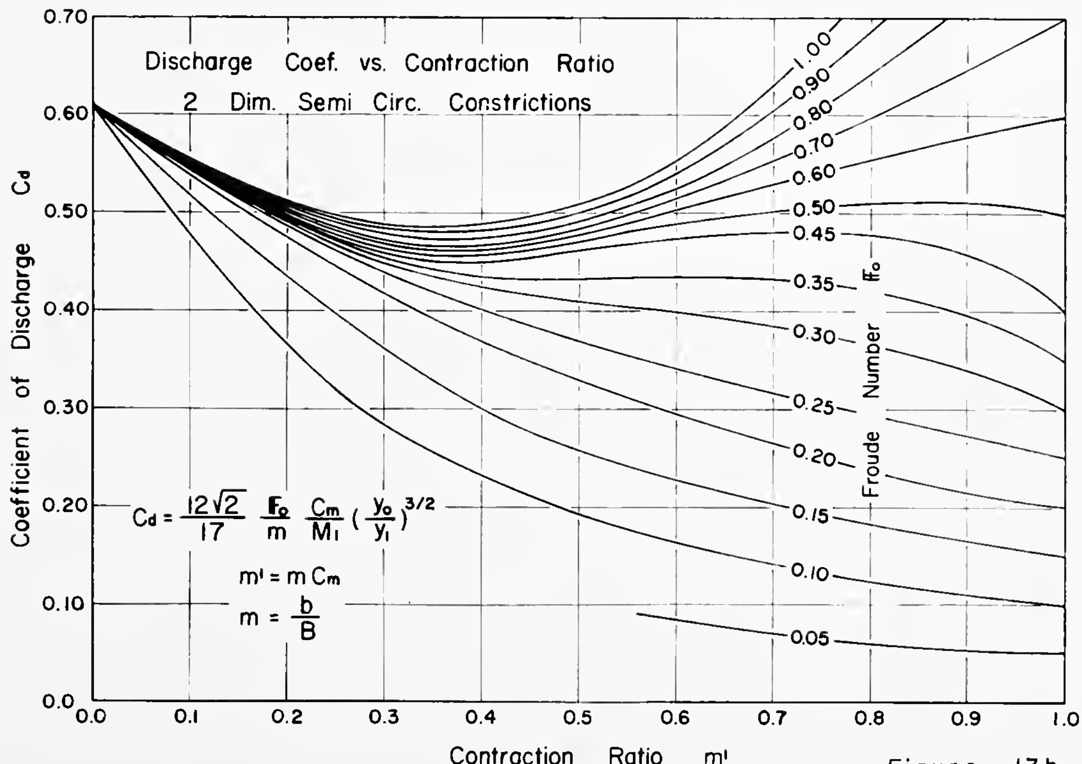

Figure 13b

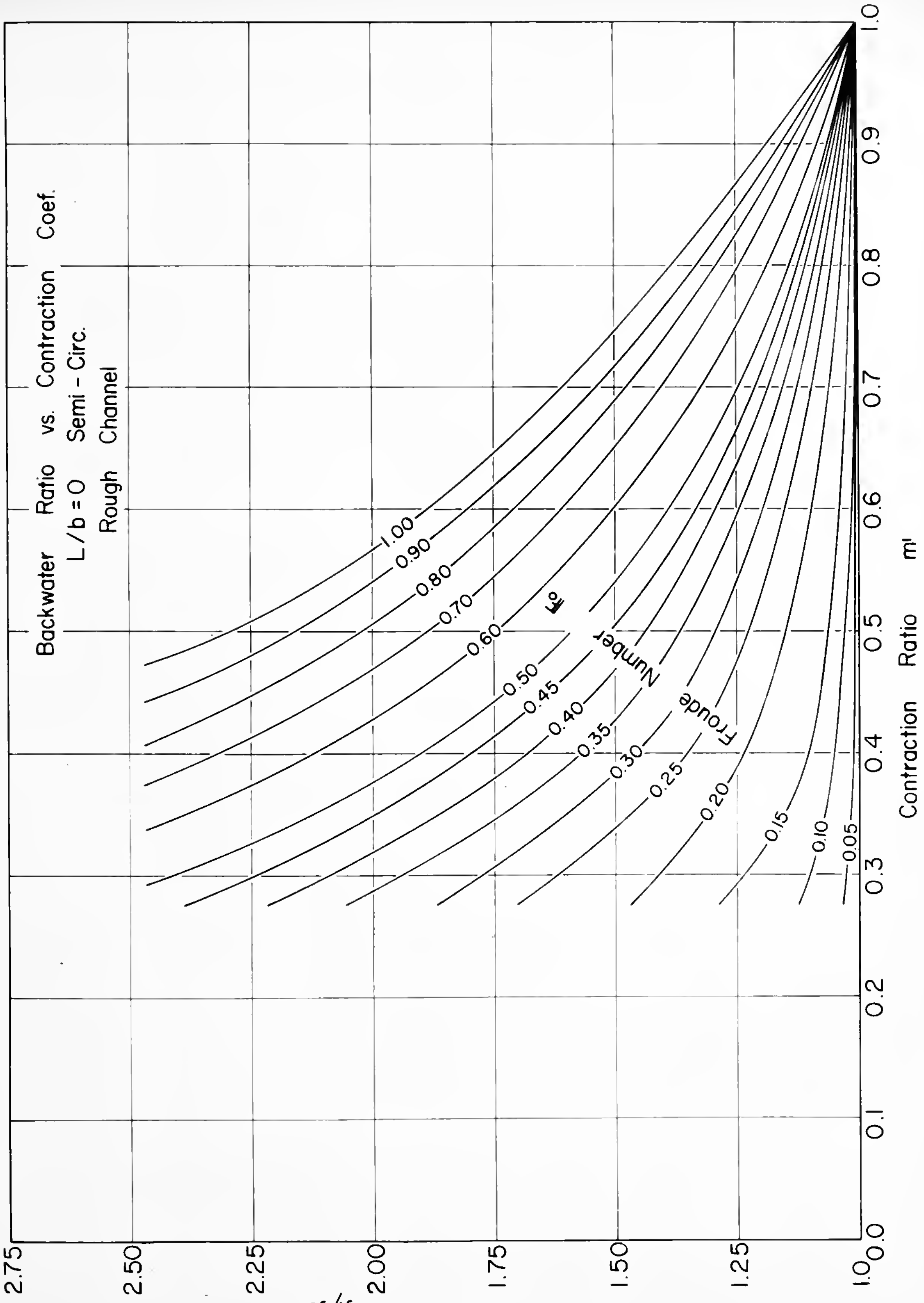
Backwater Ratio vs. Contraction Coef.
L/b = 0 Semi - Circ.
Rough Channel
Froude Number F_o
1.00
0.90
0.80
0.70
0.60
0.50
0.45
0.40
0.35
0.30
0.25
0.20
0.15
0.10
0.05
Backwater Ratio y_1/y_0
1.00
1.25
1.50
1.75
2.00
2.25
2.50
2.75
Contraction Ratio m'
0.0
0.1
0.2
0.3
0.4
0.5
0.6
0.7
0.8
0.9
1.0

Figure 14

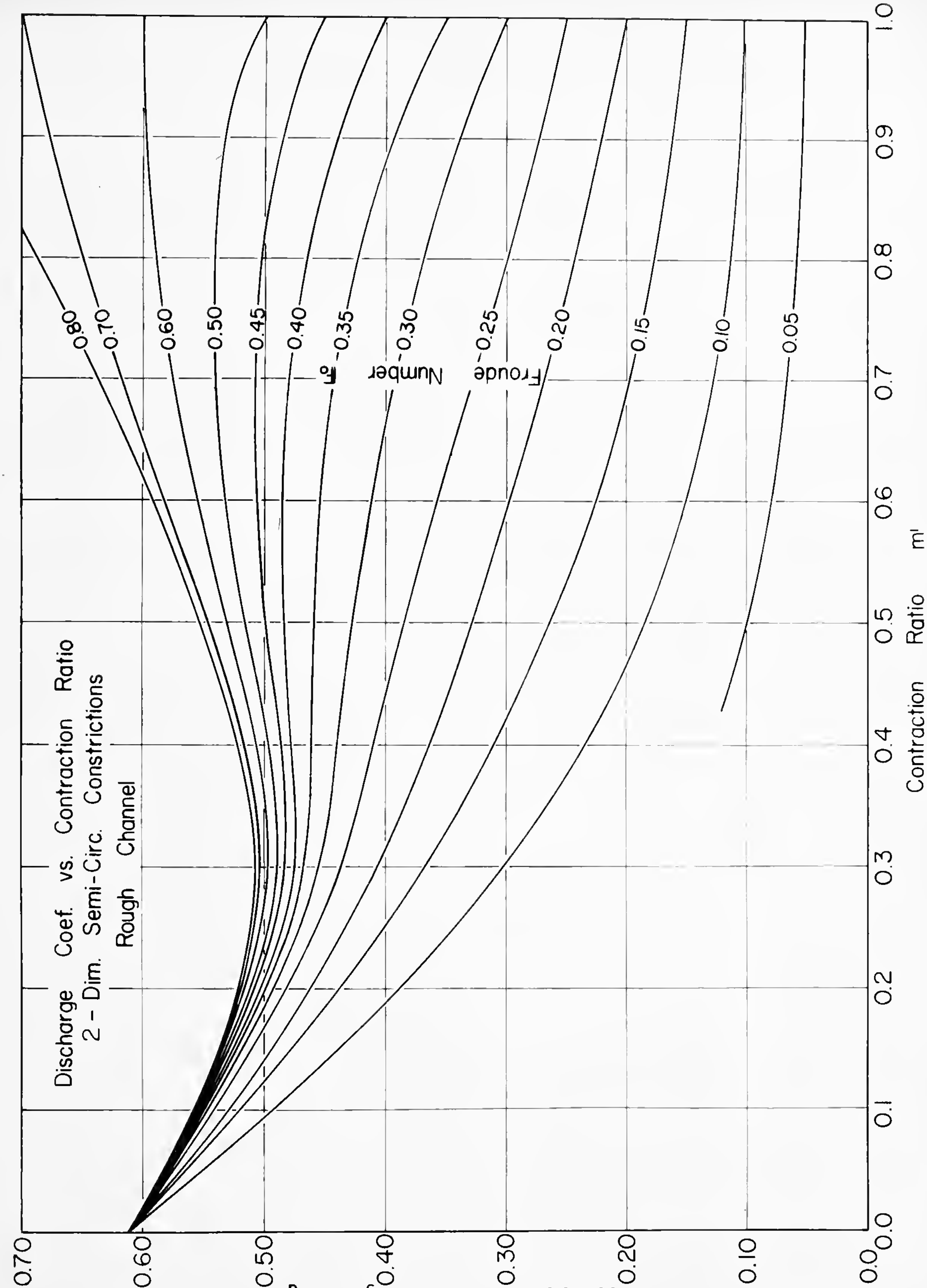
Discharge Coef. vs. Contraction Ratio
2 - Dim. Semi-Circ. Constrictions
Rough Channel
Froude Number F_0
0.80
0.70
0.60
0.50
0.45
0.40
0.35
0.30
0.25
0.20
0.15
0.10
0.05
Coefficient of Discharge C_d
0.00
0.10
0.20
0.30
0.40
0.50
0.60
0.70
Contraction Ratio m'
0.0
0.1
0.2
0.3
0.4
0.5
0.6
0.7
0.8
0.9
1.0

Figure 15

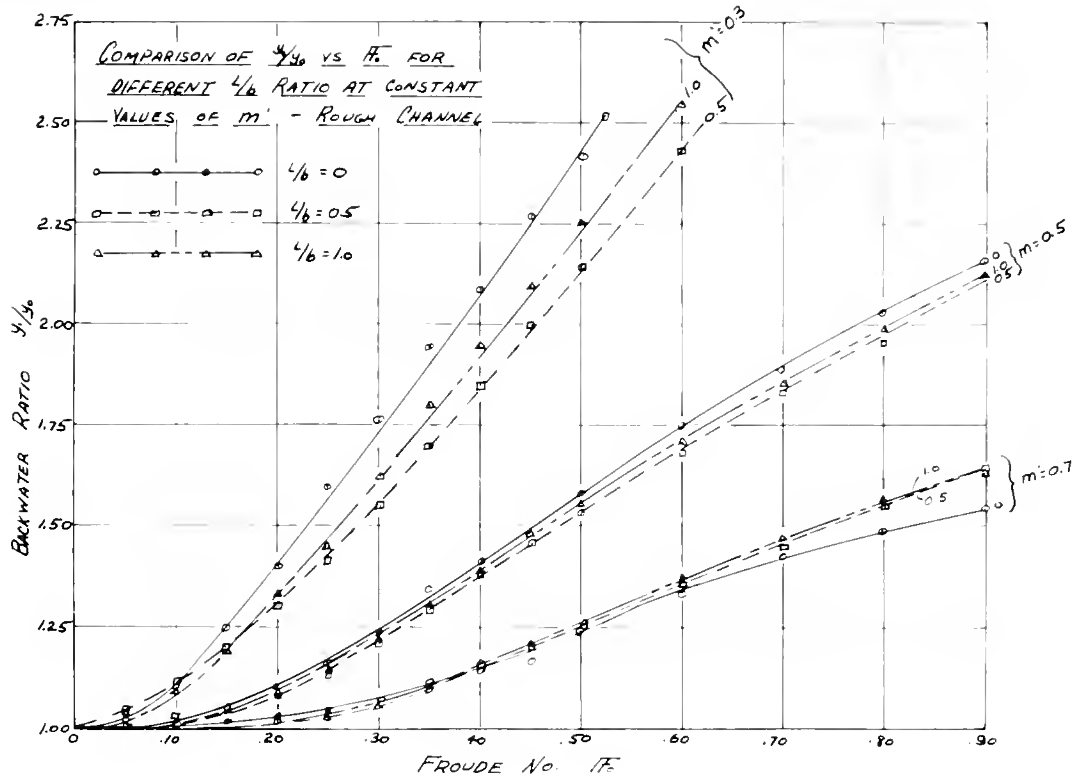

Figure 16a

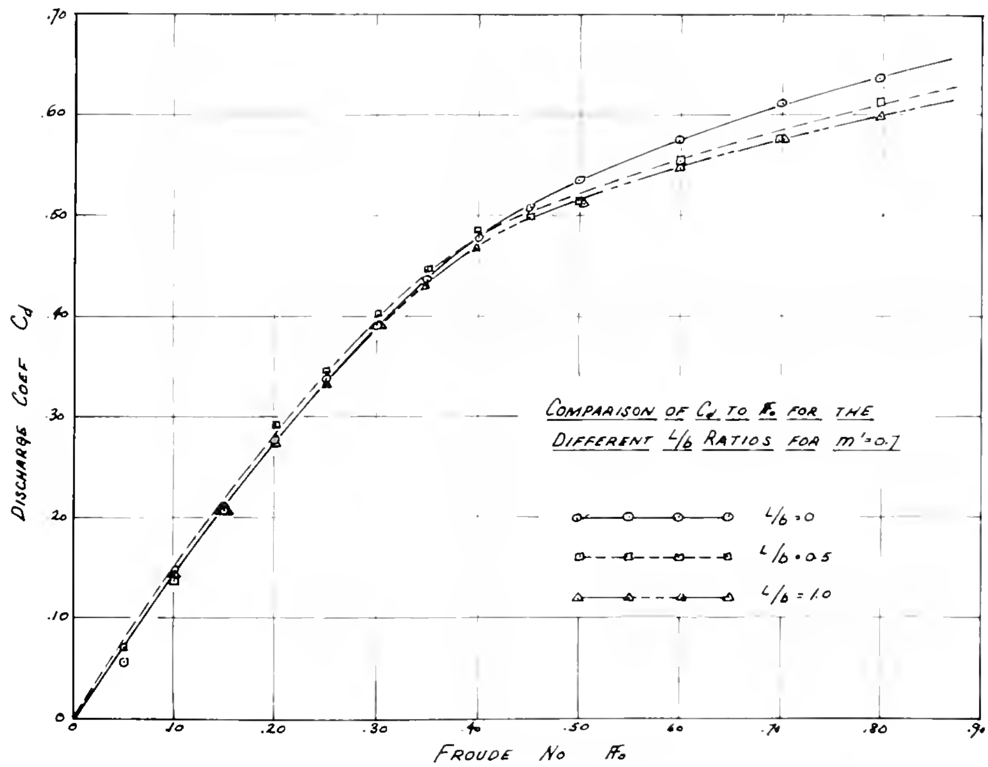

Figure 16b

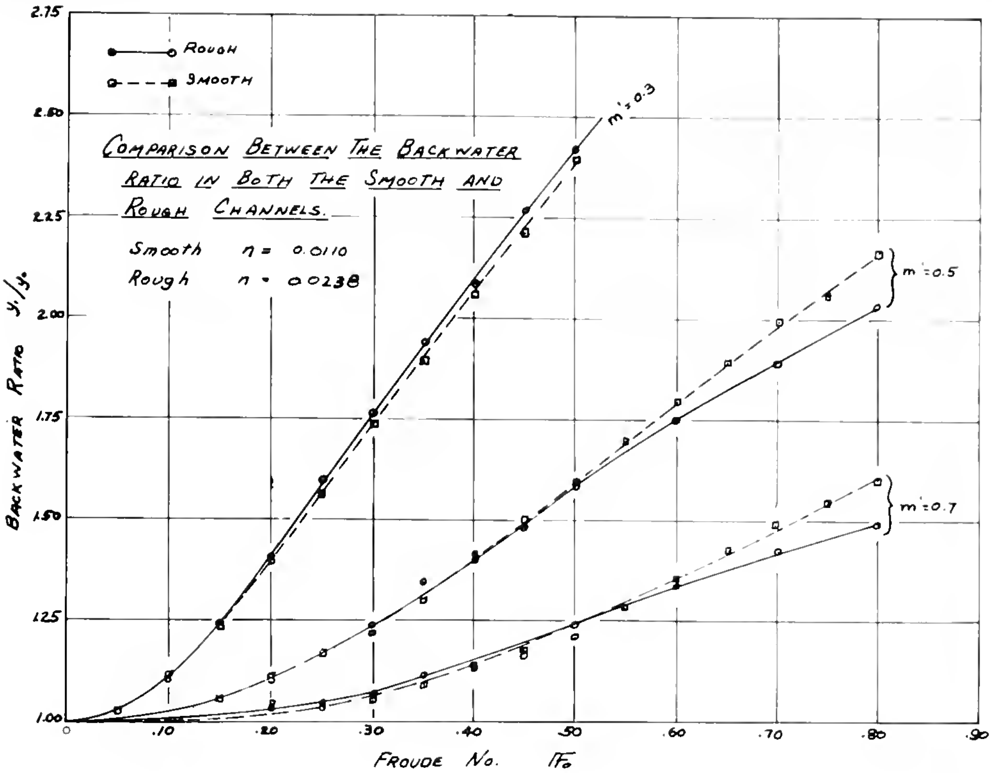

Figure 17a

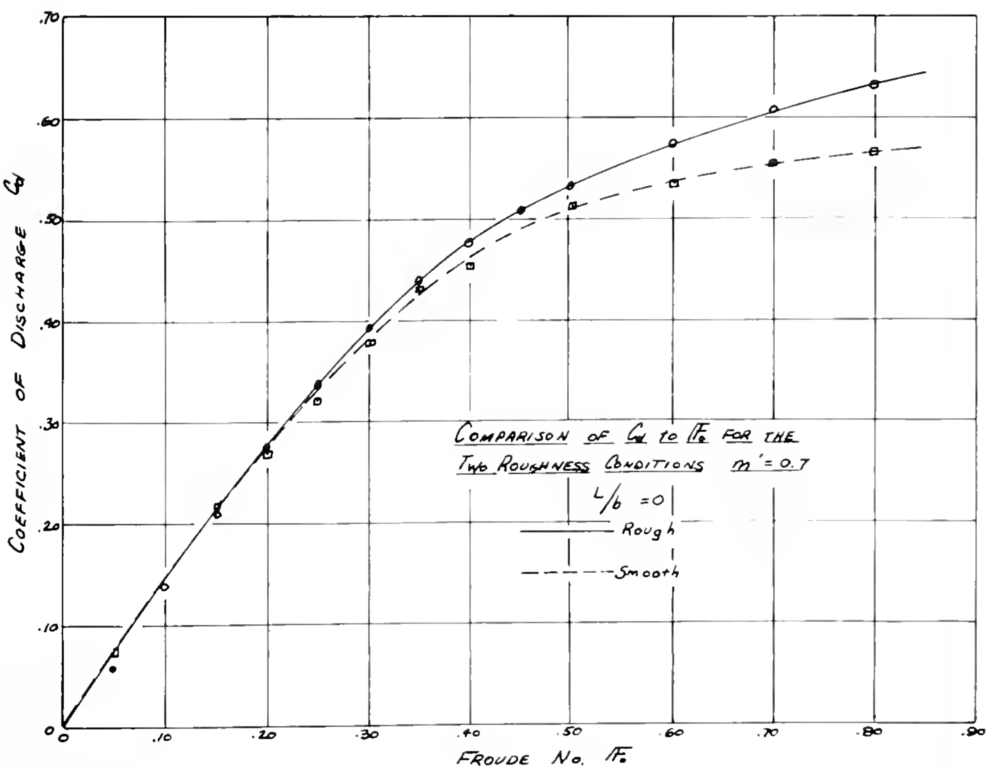

Figure 17b

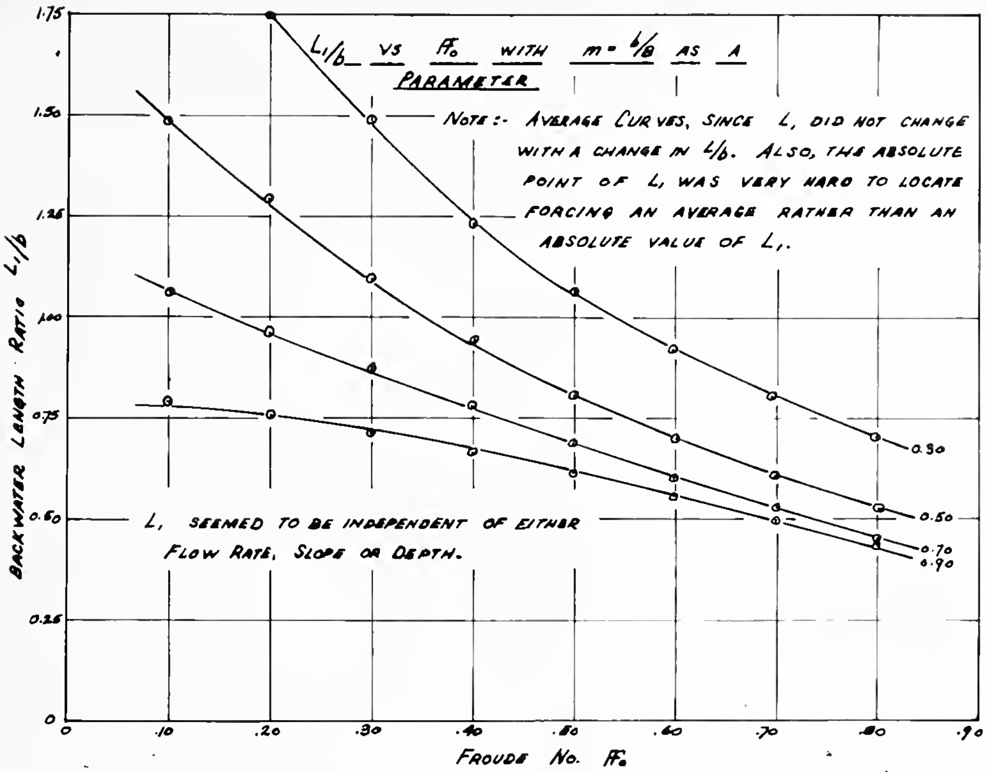

Figure 18a

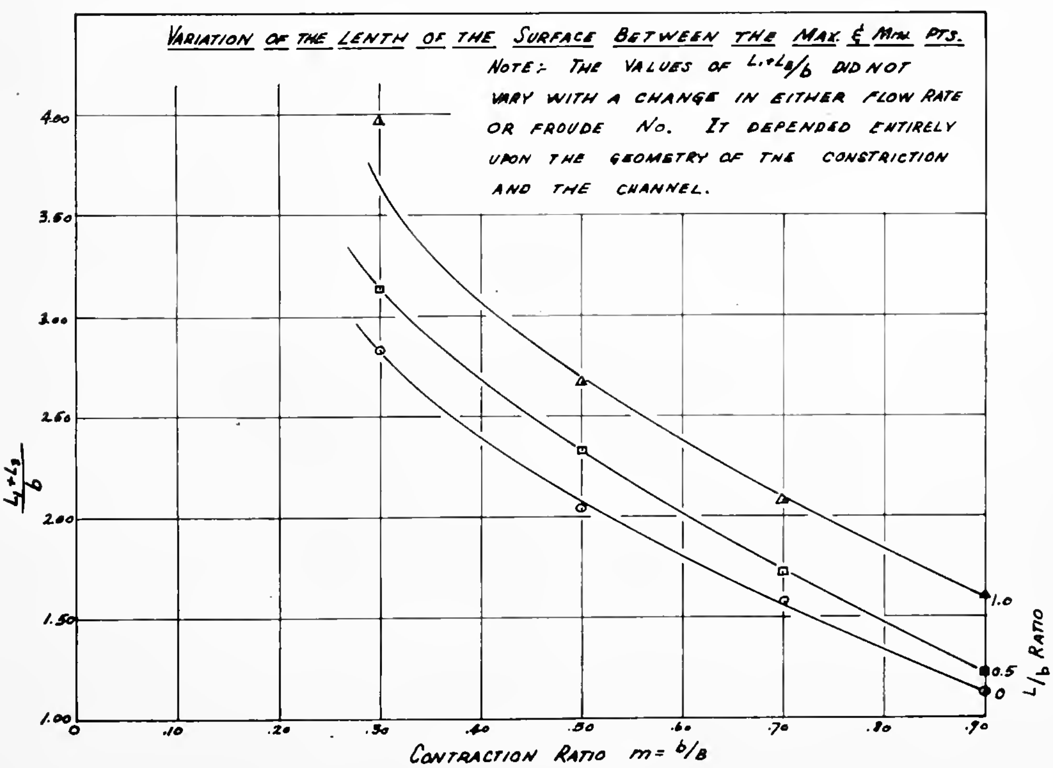

Figure 18b

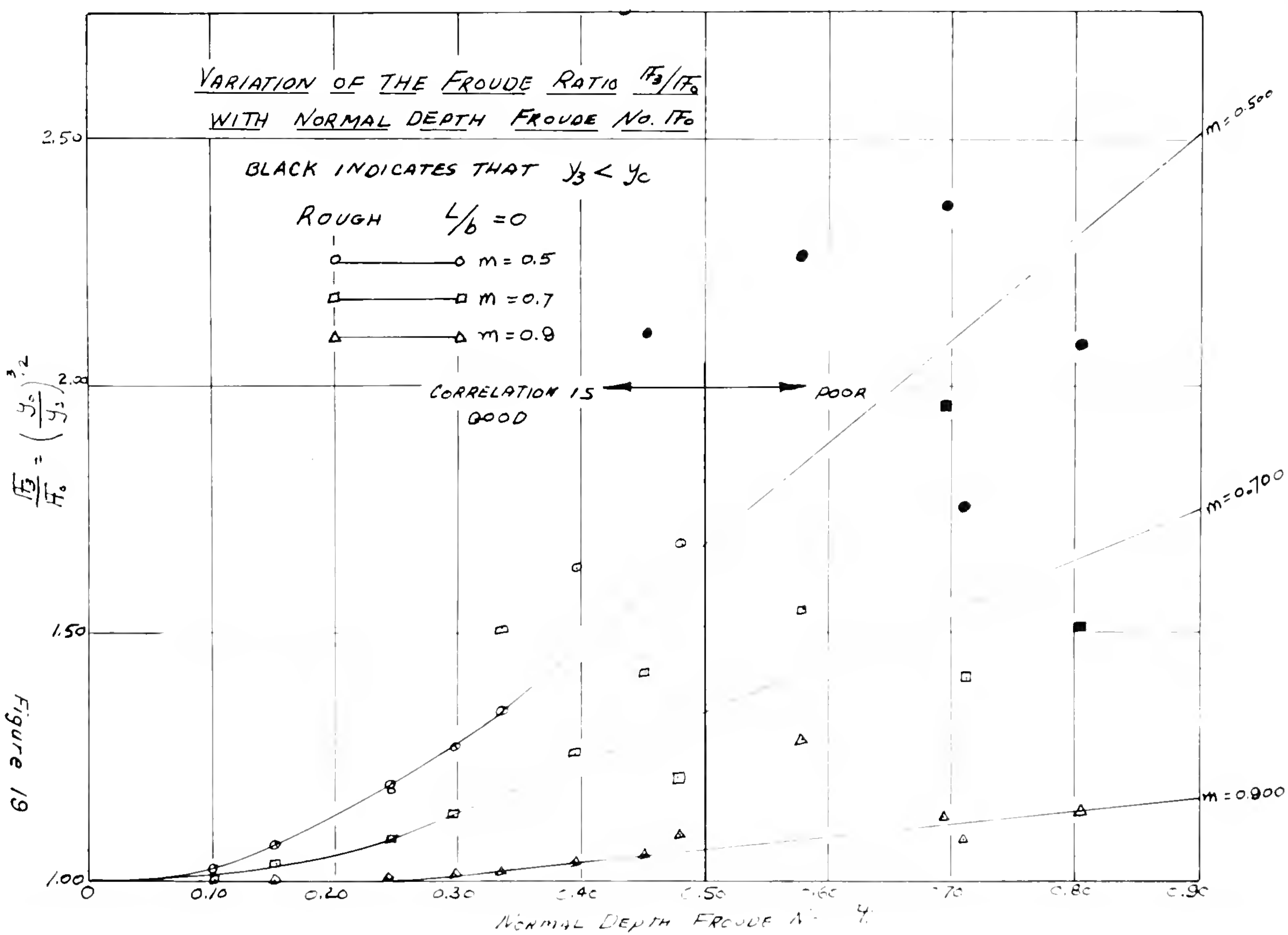

VARIATION OF THE FROUDE RATIO $\mathbb{F}_3/\mathbb{F}_0$
WITH NORMAL DEPTH FROUDE NO. $\mathbb{F}_0$
BLACK INDICATES THAT $y_3 < y_c$
ROUGH $L/b = 0$
m = 0.5
m = 0.7
m = 0.9
CORRELATION IS GOOD
POOR
m = 0.500
m = 0.700
m = 0.900
$\frac{\mathbb{F}_3}{\mathbb{F}_0} = \left(\frac{y_c}{y_3}\right)^{3/2}$
2.50
2.00
1.50
1.00
0
0.10
0.20
0.30

Figure 19

in the small preliminary flume on two-dimensional segment weirs with $\beta = d/r$ value of 0.5. (see figure). The data obtained were reanalyzed in terms of m'. These tests were run in the rough channel which had a Mannings n of 0.0201. After the results had been plotted in the form of y_1/y_0 vs. m' with $\mathbb{F}_0$ as a parameter, a comparison was made with the two-dimensional rough tests in the large flume. The results of the comparison were very good. Inspite of the fact that each set of curves had been interpolated, the small differences in the plots could easily be attributed to experimental and graphical errors.

In a similar manner, the vertical board data given by Liu[6] was reanalyzed to fit the plot of y_1/y_0 vs. m'. These tests were run in a wider flume with a different roughness pattern. Their roughness produced a Manning's n of 0.024. The results were compared to the semi-circular data and the segment data. Again the differences were extremely small and contributable to experimental error. The authors feel that it is extremely interesting to note that the test data taken by three investigators in three different flumes and under three completely different set ups produced almost identical results. This clearly verifies that as defined the contraction ratio m' is essentially an all inclusive term. Of course the data compared were those where the eccentricity was zero, the skew was zero, and the entrance was sharp. It is still necessary to apply correction terms for these conditions.

It would seem that due to the similar results mentioned above there should be some relationship between the backwater ratio y_1/y_0, the Froude No. $\mathbb{F}_0$, and the contraction ratio m'. This relationship should be applicable to all constriction geometries. As mentioned previously in the analysis, a similarity was noticed between the several different

backwater equations. The term $(\mathbb{F}_o/m')^{2/3}$ appeared in all of the solutions of y_1/y_o. In general it appeared that

$$\frac{y_1}{y_o} = C\left[\left(\frac{\mathbb{F}_o}{m'}\right)^{2/3}\right]^{\gamma} \qquad (30)$$

where C is a coefficient which would take in the effects of the discharge coefficient approach velocities, non-uniform velocity distributions and other empirically determined factors. Equation(30) is actually the equation of a straight line on logarithmic paper with a slope of γ. A total of 50 semi-circular L/b=0 test values, 44 vertical board values (Colorado[6]) and 50 segment values were plotted in the form of $y_1/y_o - 1$ vs. $(\mathbb{F}_o/m')^{2/3}$ and are shown in figure 20. The value of $y_1/y_o - 1$ was used in order to expand the scale of the backwater ratio. It is quite apparent that the data collapsed into one general straight line relationship.

The method of least squares was applied to a random sample of the 144 test points to determine the straight line relationship. After solving for γ and C, eq. (30) became

$$\frac{y_1}{y_o} = 1 + 0.469\left[\left(\frac{\mathbb{F}_o}{m'}\right)^{2/3}\right]^{3.392} \qquad (31)$$

Eq. (31) is a very simple and easy solution for the backwater produced by any type of constriction. In actual practice, this equation will give as good an estimate of the maximum backwater y_1 as any previously suggested method.

D. Surface Topography and Velocity Diagrams

In order to complete the analysis of the maximum backwater, additional studies were made of the velocity distributions and the surface profiles. These studies were made for the condition of a sharp crested semi-circular constriction with m=0.3 at a Froude No. $\mathbb{F}_o$ of 0.5.

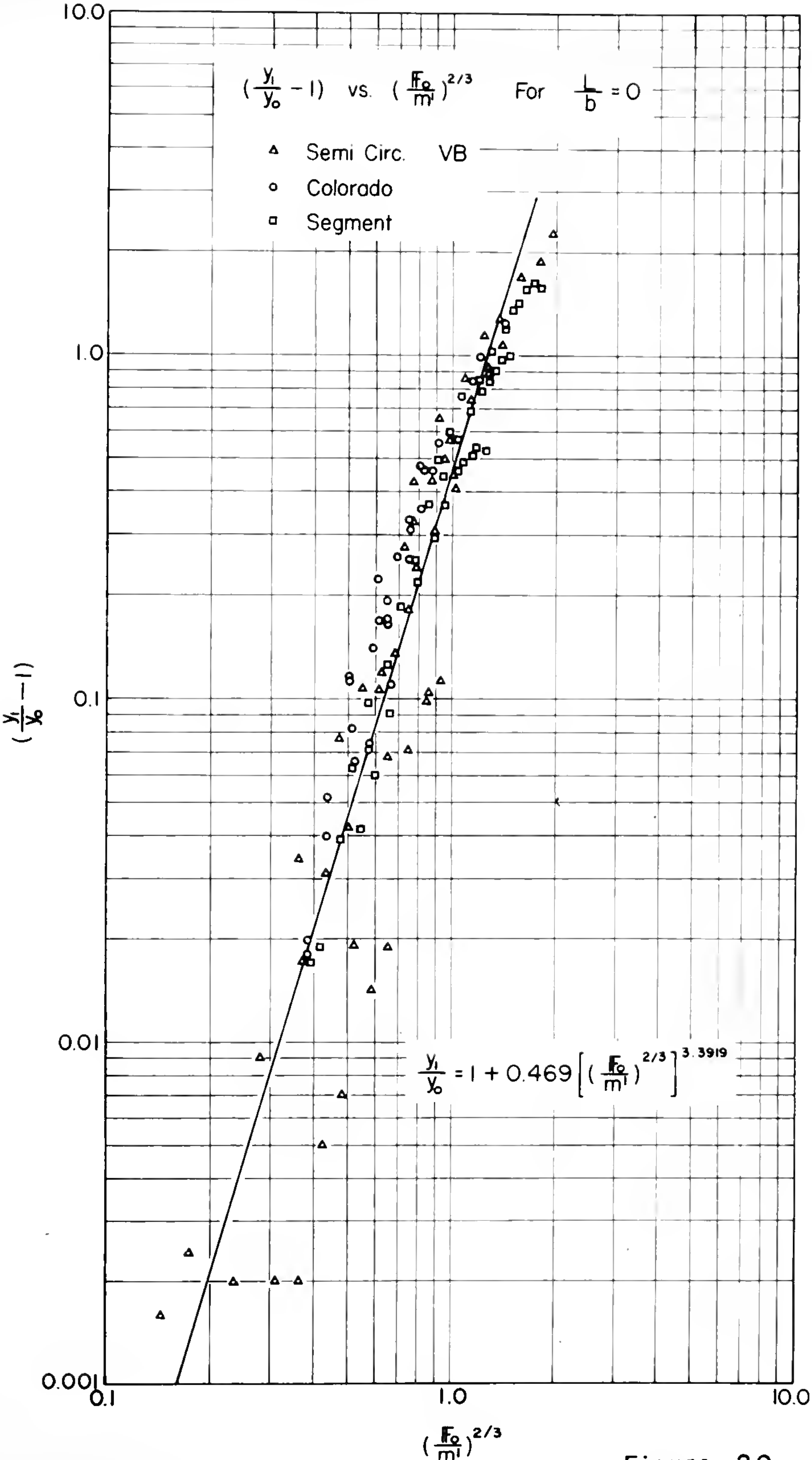
10.0
$(\frac{y_1}{y_0} - 1)$ vs. $(\frac{\mathbb{F}_0}{m'})^{2/3}$ For $\frac{L}{b} = 0$
Semi Circ. VB
Colorado
Segment
1.0
0.1
0.01
0.001
$(\frac{y_1}{y_0} - 1)$
$\frac{y_1}{y_0} = 1 + 0.469 \left[(\frac{\mathbb{F}_0}{m'})^{2/3} \right]^{3.3919}$
0.1
1.0
10.0
$(\frac{\mathbb{F}_0}{m'})^{2/3}$

Figure 20

A detail of the surface topography both upstream and downstream was observed. The result of this study is shown in figure 27. The numbers shown are the depths in centimeters. Only a detail of one half of the surface is shown since the other side is essentially symetric. The graph shows lines of equal surface elevation. The centerline surface profile is shown on the top. It is interesting to note that the actual maximum water surface elevation is not along the centerline, but on the upstream face of the abutment. Although this may be expected, the actual magnitude of the difference in elevation between the ℄ maximum elevation and the actual maximum is the important question. The actual maximum shoreline elevation was found to exceed the maximum centerline elevation by as much as 5% of the centerline depth. This fact was verified in the surface topographies taken at other conditions. Liu[6], as well as Herbich[9] gave similar surface topographies of other geometry constrictions, and the difference in water surface elevations was again found to be about 5% of the centerline depth. In general, it seems that any estimate of the maximum centerline depth y_1 should be increased by 5% to get the maximum shoreline elevation.

In addition to the surface topography, several velocity profiles were taken. Traverses were taken with the Prandtl Tube at four sections with the model m=0.3 and L/b=0 and a Froude No. F_0 of 0.5. The first section was in to backwater region of essentially uniform flow. The second was at the section of maximum backwater, the third at the vena contracta and the fourth at the section of minimum depth. At each section a vertical velocity traverse was taken at 1 ft., 2 ft. and 2.35 ft. both left and right of the centerline. At the vena contracta they were taken at the ℄, 0.5 feet and 1 foot left and right. In general, a more detailed traverse was taken at

the centerline. From these measurements, plots of equal velocity lines were prepared for the several sections. A composite picture of the isovel diagrams is shown in figure 22. Only one half of the diagrams are shown due to symetry. All of the diagrams were integrated by a planimeter and the discharge was checked against the venturi-meter discharge. They all checked within 1%. The kinetic energy coefficient α' and the momentum coefficients β' were calculated for the section of uniform flow and were found to be $\alpha' = 1.$ and $\beta' = 1.18$ respectively.

An estimate was also made of the force required by the bridge to produce the resulting backward. This was done by applying the momentum equation in the integral form between the section of maximum backwater and the vena contracta. By integrating the isovel diagrams of figure 21 and applying the momentum equation, the required bridge force was found to be 4.54 lbs. If a similar calculation is made on a similar prototype bridge with a model-prototype scale of 1/20, the bridge force would be 726,000 lbs.

CONCLUSIONS AND DESIGN RECOMMENDATIONS:

The most important variables in determining the maximum backwater are the normal depth Froude Number $\mathbb{F}_o$ and the contraction ratio m'. As defined the contraction ratio can be used for any and all types of bridge constrictions. The boundary roughness as well as the bridge length for Froude Number $\mathbb{F}_o$ less than 0.5 are relatively unimportant, and their effects for all practical purposes can be neglected. The best approximation to the backwater ratio for semi-circular arch bridges is given in figure 14. Equation(21) can be used to calculate y_1/y_o by obtaining the discharge coefficients from figure 15. A more practical first approximation to the maximum backwater is given by the curve of figure 20 or equation (31). It is

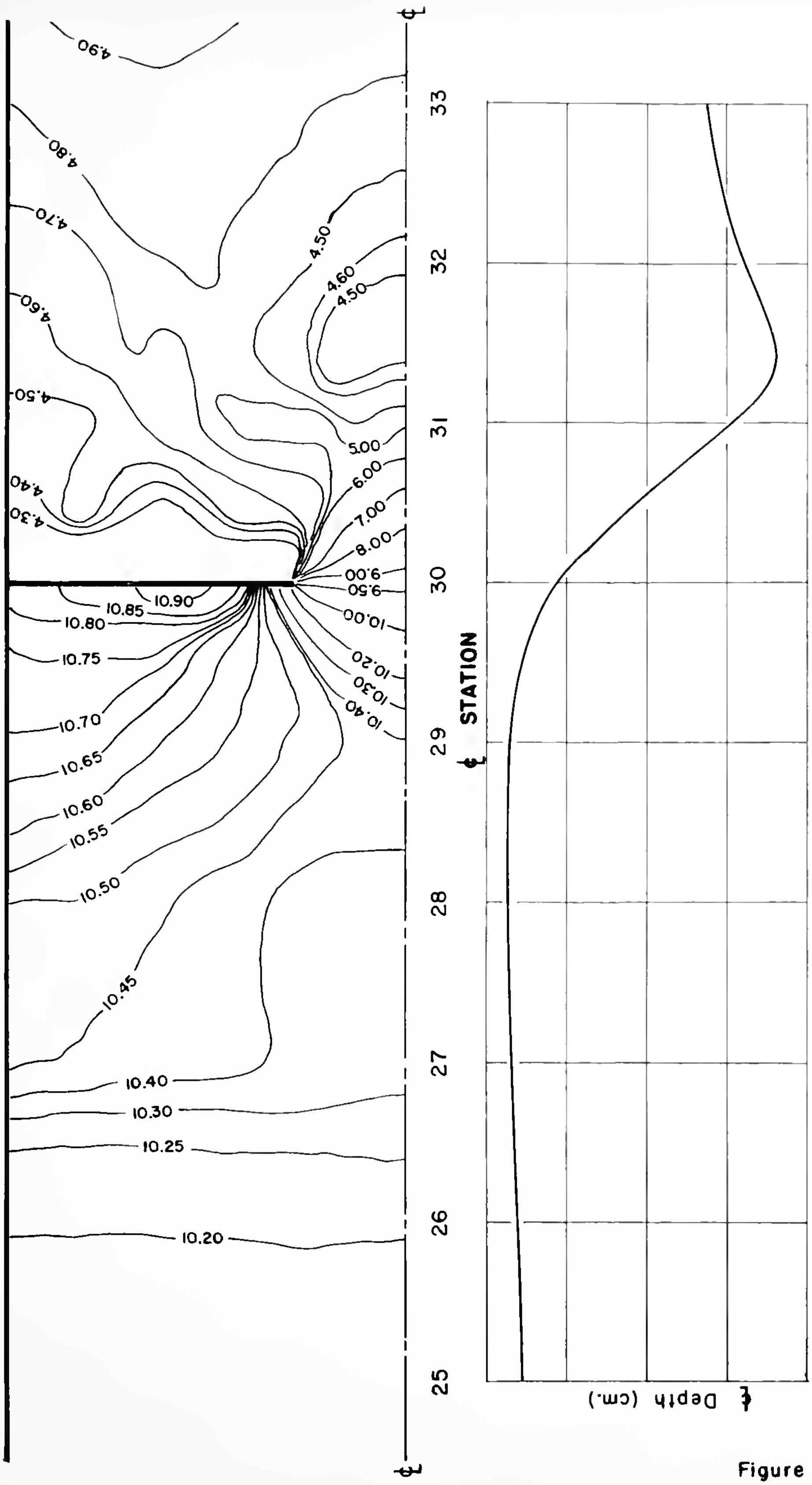

SURFACE TOPOGRAPHY

Q = 1cfs; SLOPE=0.00408; m = 0.30; L/b = 0

Figure 21

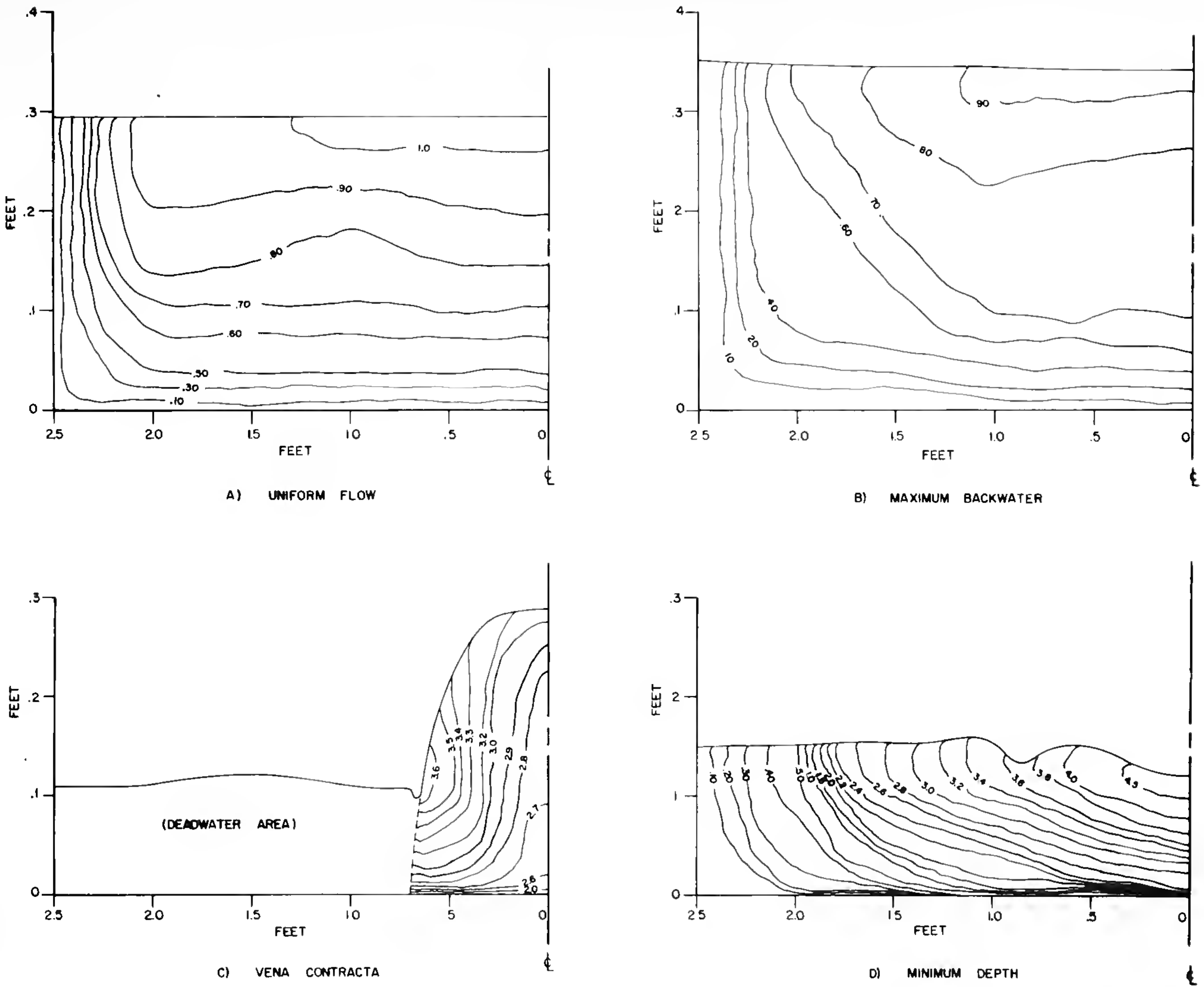

ISOVEL DIAGRAMS FOR

Q = 1 CFS ; SLOPE = .00408 ; m = .30 ; L/b = 0

FIGURE 22

recommended that 5% of this maximum depth be added to the corresponding centerline elevation to get the maximum shoreline elevation. This elevation should occur in the vicinity of the bridge embankment.

In determining the backwater produced by a new single span semicircular symmetric arch bridge where the springline of the arch is at the bed of the stream, the following design procedure is recommended.

1.) Plot the normal depth on a section view of the stream cross-section where the bridge is to be built.

2.) Superimpose the proposed bridge design on this section view.

3.) Determine the value of $m = b/B$.

4.) Calculate y_o/r and get the value of C_m from figure 3 for the curve $d/r = 0$. When the center of curvature is below the springline, calculate d/r and use the respective curve to obtain C_m.

5.) Calculate the normal depth Froude Number $\mathbb{F}_o$. (The discharge should be given and the average velocity V_o can be determined from the continuity equation.)

6.) Calculate $m' = mC_m$. (The value of m' could be checked by planimetering the areas and getting the ratio A_q/A_Q directly.)

7.) With m' and $\mathbb{F}_o$ get the value of y_1/y_o from figure 14. A more approximate value can be obtained from figure 20 or equation (31).

elev.

4.) ... the ... of ...

... from figure ... 20 ...

equation (31)

5.) Calculate the ... normal depth ...

[illegible]

determin[illegible]

[illegible]

[illegible]

[illegible]

5.) Calculate the [illegible] Number from equation [illegible]

6.) With [illegible] and [illegible] use equation 19 to get the first estimate of the discharge.

7.) With $\overline{F}_o$ and m" get the value of the discharge coefficient from figure 15. (Equation 20 can also be used.)

APPENDIX

L_1		The pe[illegible]dicular distance [illegible] the upstream face [illegible] the br[illegible] to the maximum backwater ele[illegible]ion.
L_3	L	The perpendicular distance from the upstream face of the bridge to the minimum surface elevation.

M		An infinite series of powers of the maximum depth to radius ratio.
M [illegible]		Open channel [illegible] slope [illegible] ter [illegible].
m		[illegible] ratio b/B
m		[illegible] contraction ratio
n	[illegible]	[illegible] roughness coefficient.
[illegible]	L^3T^{-1}	[illegible]
q	L^3T^{-1}	[illegible] of the [illegible] flow [illegible] could pass through the bridge without contraction.
R	L	Hydraulic radius.
R_o		Reynolds number [illegible]
R_q		Reynolds number [illegible]
r		Radius of the [illegible].
$y_{[illegible]}$	[illegible]	Depth of normal [illegible] flow.
$y_{[illegible]}$	[illegible]	Depth of the maximum backwater.
$y_{[illegible]}$	[illegible]	Depth at the [illegible] contraction.
$y_{[illegible]}$	[illegible]	Depth at the [illegible] surface elevation.
[illegible]		Symbol for the ratio y_o/r.
α'		Kinetic energy coefficient.
β		Symbol for the ratio d/r.
β'		Momentum coefficient.
ν	L^2T^{-1}	Kinematic viscosity of the fluid
ρ	FT^2L^{-4}	Fluid mass density.
τ_o	FL^2	Shear intensity acting on the channel bed.
χ	L	Roughness parameter suggested by Sayre.